Symmetric Colour Vision Model LMSLAB for Elementary Colours and Chromatic Adaptation

Presented: Workshop at FARBINFO '06, TU Dresden, September 30, 2006

Prof. Dr. Klaus Richter, BAM and TU Berlin
Federal Institute for Materials Research and Testing (BAM), VIII.1
Unter den Eichen 87, D-12200 Berlin
Tel. +49 30 8104 1834; Fax +49 30 8104 1807

Version 1.2: 2007-08-15

klaus.richter@bam.de

See web site of Project Group VIII.34, Visual Methods and Image Reproduction

http://www.ps.bam.de

For the latest German and English versions of this paper, see (1,5 MByte, 28 pages)

http://www.ps.bam.de/VISG06.PDF

http://www.ps.bam.de/VISE06.PDF

Abstract

A symmetric model of static colour vision with logarithmic responses of the three cones *P, D* and *T* (or *L, M*, and *S*) is described. The cone distribution ratio which is approximately *P:D:T* = 1:2:16 leads to a spectral sensitivity of the "blue" cone T which is 16 times larger compared to the spectral sensitivity of the "red" cone P. This property leads to three logarithmic sensitivities *U, N* and *W*. The three sensitivities *P, D, T* have the maxima at 435, 540 and 570 nm and the three further sensitivities *U, N, W* have the maxima at 555, 495 and 525nm. All six have a parable form of the same shape. The maxima and shape of *U*, and *N* are similar to the maxima and shape of photopic vision *V(λ)* and scotopic vision *V'(λ)* The logarithmic response ratio of any two sensitivities is a straight line as function of wavelength. The logarithmic ratios of two sensitivities, for example log *(P/U)*, log *(P/N)* are called "excitations".

In application the "cone excitation diagrams" have a spectral locus and are different logarithmic transformations of the standard CIE *(x, y)* chromaticity diagram.The axis of the "cone excitation diagrams" are defined by the spectral location of the four elementary colours Yellow (J), Green (G), Blue (B), and Red (R) with spectral locations near 575, 525, 475 and 494c nm (on the purple line). All excitation diagrams for example with the axis *a'* = log *(P/W)* and *b'* = log *(U/W)* in red–green and yellow–blue direction are similar to the non linear chromaticity diagram *(a', b')* defined by Richter (1980) for CIELAB. If chromatic adaptation is assumed by a linear shift between the sample and the background excitation then many experimental chromatic adaptation results can be described, for example the *Evans* (1974) G0-colours for three spectral backgrounds (475, 528 and 608 nm) of equal luminance. The "*von Kries* theory of chromatic adaptation" can not describe these chromatic adaptation data as well as the new chromatic adaptation model.

1. Introduction

1.1 Receptor sensitivities in a linear and log plot

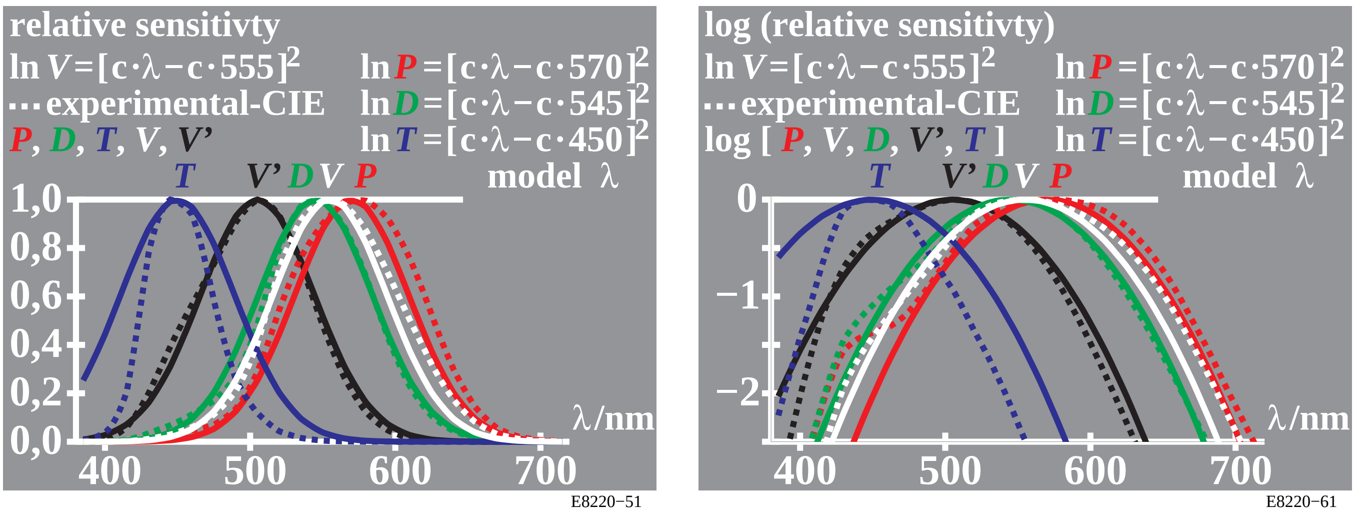

Figure 1: Three cone sensitivities *P(λ)*, *D(λ)*, *T(λ)* and photopic and scotopic sensitivity *V(λ)* and *V'(λ)*

Fig. 1 shows the three cone sensitivities *P(λ), D(λ), T(λ)* and photopic and scotopic sensitivity *V(λ)* and *V'(λ)* in a linear *(left)* and logarithmic *(right)* plot as function of wavelength. The *Gaussian* shape in the linear plot is transferred to a parable of approximately the same shape in the logarithmic plot. All sensitivities are normalized to one in the linear *(left)* and to zero in the logarithmic *(right)* plot. In the following an index o, for example $P_o(\lambda)$, is used for this normalization and an index a, for example $P_a(\lambda)$, is used for some kind of adaptation (a) which changes the zero-normalization in the log plot to other values.

1.2 Conflicting terms and use of PDT instead of LMS in this paper.

Recently the publication CIE170-1:2006 includes for the first time the three cone sensitivities *L, M,* and *S*. Unfortunately the two groups of CIE division I "Colour and Vision" have defined the same letters *L, M, S* for different terms. For a long time the "colour" section is familiar with luminance *L*, the relative luminance $L_r = L/L_b$ (b = background), the lightness *L**, and the relative lightness *l**, see for example ISO/IEC 15775. Additionally colourfulness *M* and saturation *S* are familiar terms.

The many didactic problems, for example in the recent book "Light, Vision, Colour" of *Valberg* (2005) which shows for example the "cone responses *L*" in "luminance (photopic) units *L*" have to be avoided. Therefore for the three cones in this paper the often used symbols ***P, D,*** and ***T*** (for ***P****rotanopic*, ***D****euteranopic*, and ***T****ritanopic* vision) are used instead of *L, M,* and *S* (for the cones in the Long, Medium and Short wavelength range).

The new *LMS* cone data (CIE 170-1:2006) have maxima near 570, 540 and 445nm and are not normalized to one in the linear mode. The colour vision model of this paper uses the wavelength 435 instead of 445 for the maximum of the "blue" cone *T*. This gives a better approximation for the wavelengths larger 450nm. The short wavelength approximation is of much less importance because of the low transmission (<1%) of the optical eye media for all wavelength below 380nm

1.3 Three basic sensitivities *PDT*, three calculated sensitivities *UNW and excitation*

The three sensitivities *P, D, T* with maxima at 435, 540 and 570 nm and the three model sensitivities *U, N* and *W* with maxima at 555, 495 and 525nm have a parable form in a logarithmic plot. The maxima and shape of *U, N, W* is similar to the maxima and shape of photopic vision ***V(λ)***, of scotopic vision ***V'(λ)*** and of the logarithmic mean of both, which is called the shape of "mesopic" vision in this paper. Then the logarithmic response ratio (or log difference) of any two of the six sensitivities is always a straight line as function of wavelength. The logarithmic ratios of two sensitivities, for example *log (P/U)*, *log (P/N)* or *log (P/W)* are called "excitation". If these ratios are plotted in two appropriate dimensions for example in Red-Green and Yellow-Blue direction, then "cone excitation diagrams" in photopic, scotopic or mesopic units are defined.

1.4 Receptor sensitivities and excitations

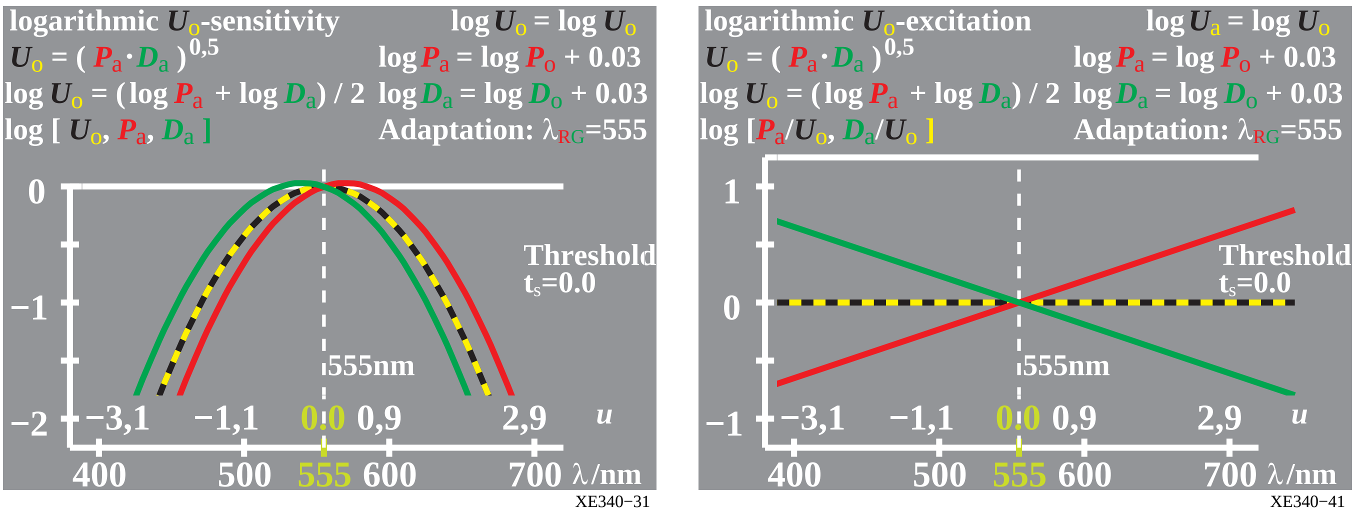

Figure 2: Cone sensitivities log $P_a(\lambda)$, log $D_a(\lambda)$ *and cone excitations* log [$P_a(\lambda) / U_o(\lambda)$] and log [$D_a(\lambda) / U_o(\lambda)$]

Fig 2 shows the cone sensitivities log $P_a(\lambda)$, log $D_a(\lambda)$ and cone excitations log [$P_a(\lambda) / U_o(\lambda)$] and log [$D_a(\lambda) / U_o(\lambda)$] as function of wavelength λ. Because of the same parable shape of the two cones both cone excitations are straight lines. Instead of the wavelength λ a more usual parameter *u* in the range -3 to +3 can be used which is defined in Fig. 4. The parameter *u* can additionally describe the two parables and the two straight lines.

Half of the logarithmic sum of the two cone sensitivities $P_a(\lambda)$ and $D_a(\lambda)$ is called $U_o(\lambda)$. This curve is in shape, maximum and value very similar to the photopic sensitivity $V(\lambda)$, compare Fig. 1. The deviation of $U_o(\lambda)$ is less than 1% compared to $V(\lambda)$ at 400 and 700 nm, compare Richter (1996).

For the luminance adaptation to the usually white or grey background there is a limited dynamic range for each receptor response which is near 1% of the maximum. The exact value can be measured by threshold experiments and decreases to 0,5% with increasing luminance L in the photopic range between 100 and 20.000 cd/m^2. In the next Fig. 3 examples are plotted for the threshold values t_s = 0.007 (0,7%). Then the cone excitations decrease at both ends of the spectral range.

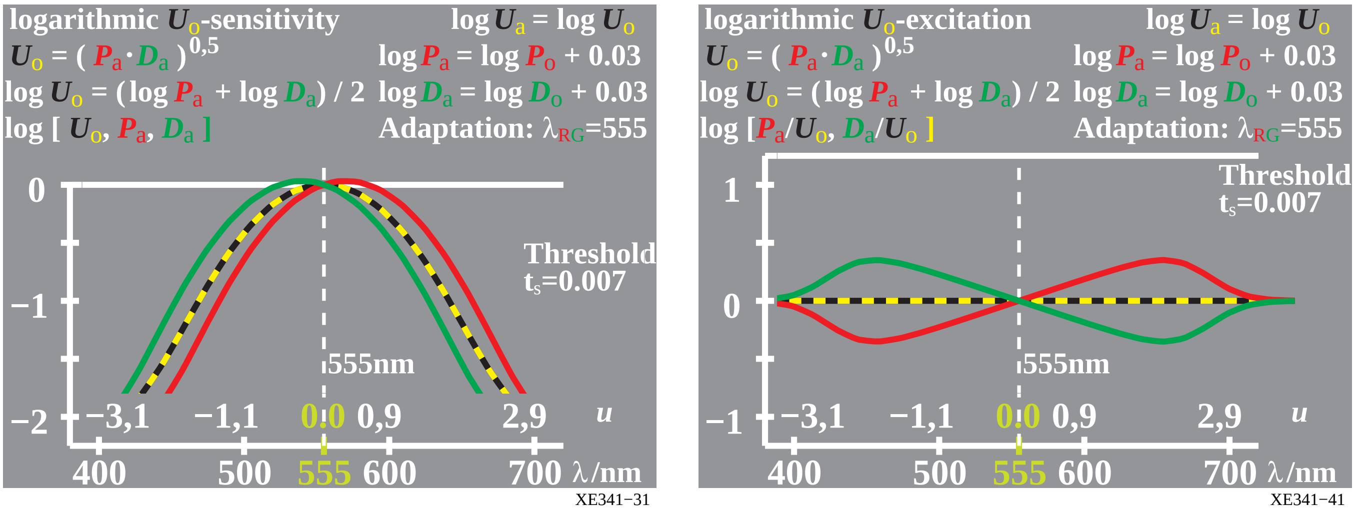

Figure 3: Cone sensitivities log $P_a(\lambda)$, log $D_a(\lambda)$ *and cone excitations* log [$P_a(\lambda)$ / $U_o(\lambda)$] and log [$D_a(\lambda)$ / $U_o(\lambda)$]

Fig 3 shows the cone sensitivities log $P_a(\lambda)$, log $D_a(\lambda)$ and cone excitations log [$P_a(\lambda)$ / $U_o(\lambda)$] and log [$D_a(\lambda)$ / $U_o(\lambda)$] as function of wavelength λ for a dynamic cone range with a threshold value t_s = 0.007. Similar properties are expected for other cone combinations.

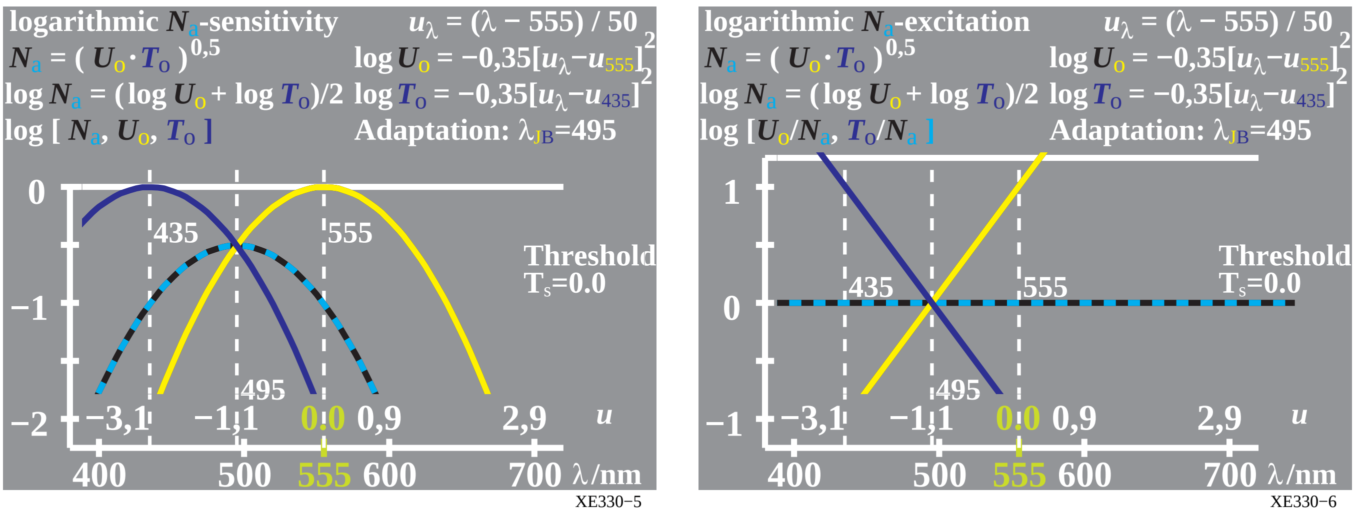

Figure 4: Sensitivities log $T_o(\lambda)$, log $U_o(\lambda)$ and log $N_a(\lambda)$ *and excitations* log [$T_a(\lambda)$ / $N_a(\lambda)$], log [$U_o(\lambda)$ / $N_a(\lambda)$]

Fig 4 shows the sensitivities log $T_o(\lambda)$, log $U_o(\lambda)$, and log $N_a(\lambda)$ and excitations log [$T_o(\lambda)$ / $N_a(\lambda)$] and log [$U_o(\lambda)$ / $N_a(\lambda)$] as function of wavelength λ. Because of the same parable shape of the two "cones" both excitation are a straight line. Instead of the wavelength λ a more usual parameter u in the range –3 to +3 can be used which is defined in the figure. The parameter u can describe the two parables and the two straight lines.

Half of the logarithmic sum of the two sensitivities $T_o(\lambda)$ and $U_o(\lambda)$ is called $N_a(\lambda)$. This curve is in shape, maximum and value very similar to the scotopic sensitivity $V'(\lambda)$, compare Fig. 1. In the next Fig. 5 instead of the threshold value t_s = 0 the value t_s = 0.007 (0,7%) is used. Then the cone excitation decreases at both ends of the spectral range.

The dynamic range for the achromatic threshold is near 1%. But for the chromatic threshold especially for blue colours the dynamic range seem to be two log units below the value for achromatic colours. We have to discuss this later again. In the next Figure at a first assumption still the threshold value t_s = 0.007 (0,7%) is used which changes the shape of the sum and the excitation very much compared to Fig. 4.

The large slope of the two cone excitations indicates a value only in a limited spectral range for the visual system. There seem to be a visual method to reduce the slope by a factor two for any sample in a background. This increases the spectral range by a factor 2.

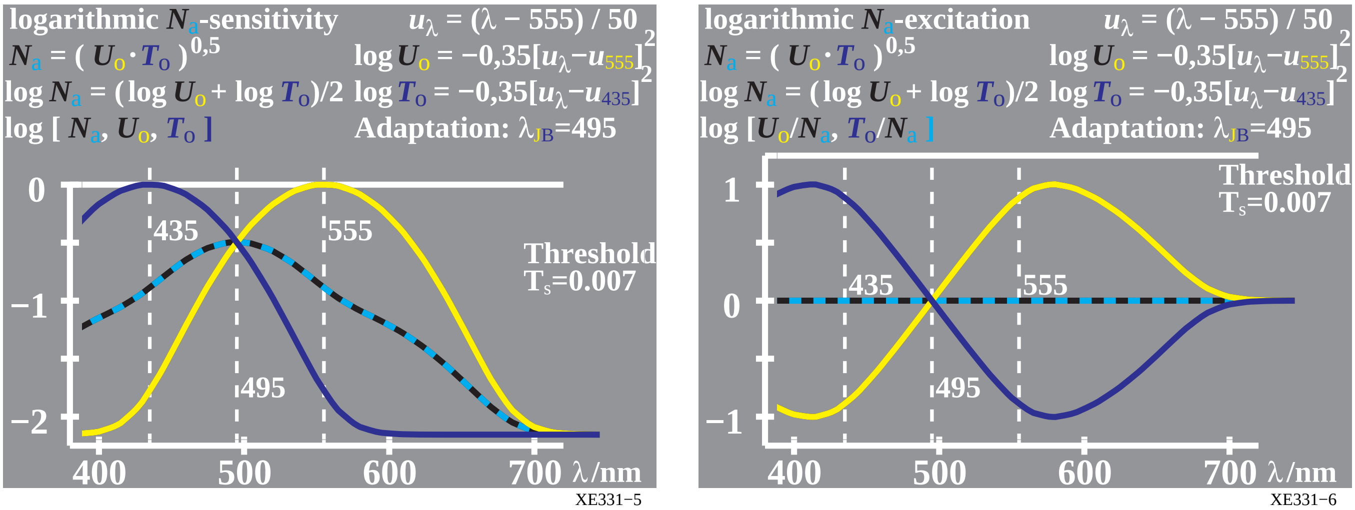

Figure 5: Sensitivities log $T_o(\lambda)$, log $U_o(\lambda)$ and log $N_a(\lambda)$ and excitations log [$T_o(\lambda)$ / $N_a(\lambda)$], log [$U_o(\lambda)$ / $N_a(\lambda)$]
Fig 5 shows the sensitivities log $T_o(\lambda)$, log $U_o(\lambda)$ and log $N_a(\lambda)$ and excitations log [$T_o(\lambda)$ / $N_a(\lambda)$] and log [$U_o(\lambda)$ / $N_a(\lambda)$] as function of wavelength λ for a dynamic cone range with a threshold value t_s = 0.007. Similar properties are expected for other sensitivity combinations.

2. Reasons for a symmetric model of colour vision

2.1 Symmetric excitation as function of wavelength

The excitations in Fig. 2 to Fig 5 *(right side)* are symmetric compared to the zero line for all wavelength. Additionally there is a symmetry on the wavelength scale for the RG-process at 555nm and for the BJ-process at 495nm.

Therefore there are symmetric properties in colour vision and the role of this symmetry in vision has to be discussed.

2.2 Complementary optimal colours and the *Holtsmark-Valberg* threshold results

In 1969 *Holtsmark* and *Valberg* published the results for colour thresholds of complementary optimal colours. Such complementary optimal colours are known from black and white borders which are viewed by a prism. The German poet *Goethe* has first described the complementary colours and their discrimination around 1800.

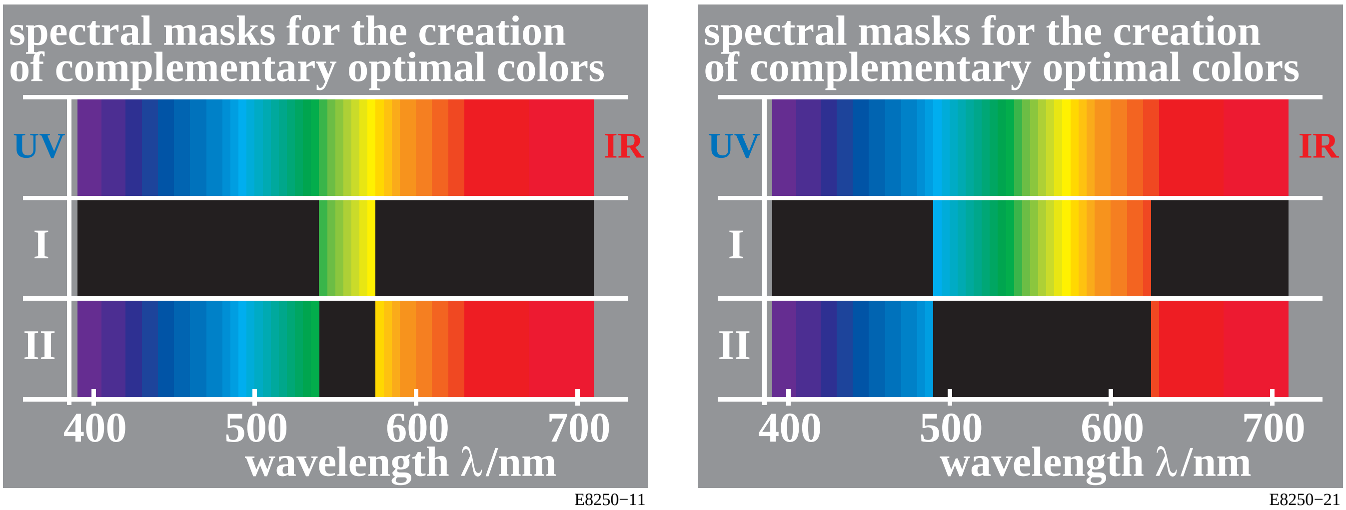

Figure 6: Spectrum, complementary optimal colours and the *Valberg–Holtsmark* thresholds
Fig. 6 shows the spectral colours of equal radiation. The mixture of all spectral colours leads to the colour “white” and the mixture of different continuous parts leads to the so called optimal colours. On the left side a small band leads to a dark optimal colour (part I) and a large band leads to a light optimal colour (part II). Both colours are complementary and the two mix together to white. On the right side the complementary optimal colours have about equal bandwidth on a wavelength scale.

Holtsmark and *Valberg* (1969) produced at first two adjacent and equal optimal colours in a white background with two equal black masks shown in Fig. 6. By movement of one of the black masks one optimal colour was changed (mainly in hue) and the threshold was determined. For this threshold the necessary mask movement was the same for complementary optimal colours and six observers.

Holtsmark and *Valberg* calculate from the results the wavelength discrimination of complementary optimal colours. The wavelength discrimination at threshold was approximately the same. We have to explain this result by colorimetric calculations and physiological models, for an experimental example see (5 MByte)

http://www.ps.bam.de/CIE63/HV01.PDF

The *Holtsmark* and *Valberg* results define a **symmetric structure for a colour threshold formula** which must calculate the same difference at least for the hue discrimination which is here the main change in the experiments.

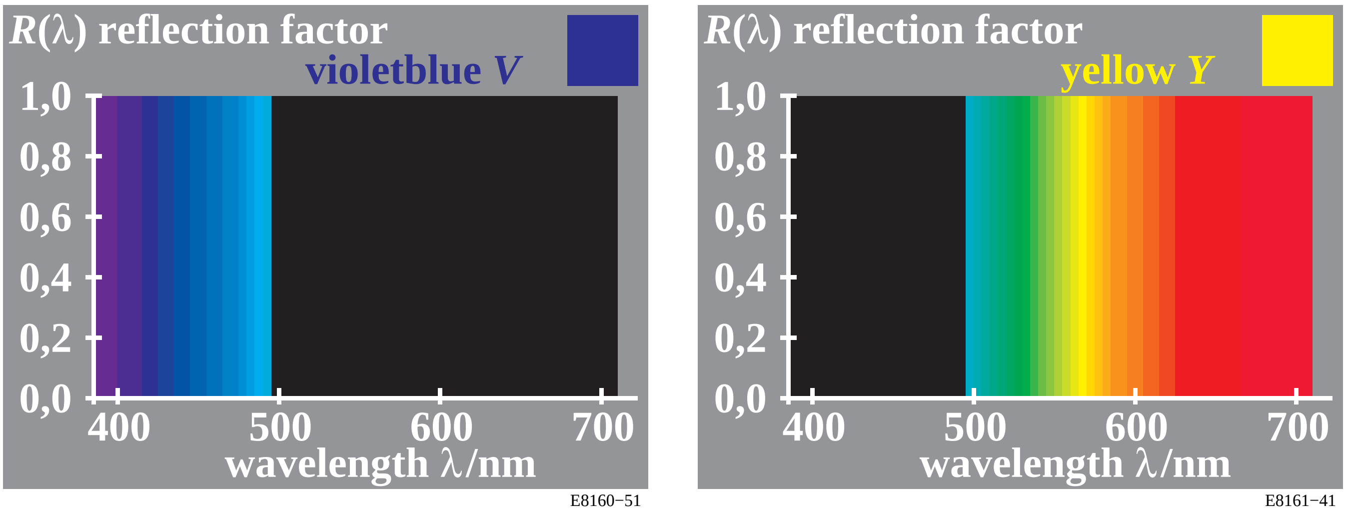

Figure 7: Complementary optimal colours Violet blue V and Yellow Y
Fig. 7 shows two complementary optimal colours Violet blue V and Yellow Y. The names are defined in ISO/IEC 15775. The change of the reflection for a good three colour reproduction system is near 490 nm and 590 nm. Among the optimal colours are the most chromatic and most light colours. In the following we will give the CIE tristimulus values for the three basic optimal colours OLV and the three mixed optimal colours CMY.

basic and mixed additive optimal colors for illuminant D65					
basic color or mixed color and name	**CIE standard chromaticity**		**CIE standard tristimulus value**		
	x	***y***	***X***	***Y***	***Z***
three additive basic optimal colors:					
O orange red	0,6695	0,3302	42,65	21,04	0,02
L leaf green	0,2991	0,6351	34,87	74,04	7,67
V violet blue	0,1445	0,0393	18,06	4,90	102,02
three additive mixed optimal colors:					
C cyan blue	0,2191	0,3268	52,94	78,96	109,70
M magenta red	0,3218	0,1375	60,73	25,95	102,04
Y yellow	0,4300	0,5274	77,53	95,09	7,69
D65 (white)	0,3131	0,3275	95,60	100,00	109,71

E8581–

Figure 8: Complementary optimal colour data CIE *(x, y)* and *XYZ*

Fig. 8 shows the data CIE *(x, y)* and *XYZ* for the optimal colours *OLV* and the complementary optimal colour *CMY.*

basic and mixed additive optimal colors 01 normalized for D65					
basic color or mixed color and name	**Range 01 normalized chromaticity**		**Range 01 normalized tristimulus value**		
	x_{01}	y_{01}	$X_{01}=X/X_n$	$Y_{01}=Y/Y_n$	$Z_{01}=Z/Z_n$
three additive basic optimal colors:					
O orange red	0,6792	0,3304	0,4461	0,2105	0,0002
L leaf green	0,3102	0,6295	0,3649	0,7405	0,0709
V violet blue	0,1620	0,0420	0,1890	0,0490	0,9289
three additive mixed optimal colors:					
C cyan blue	0,2364	0,3369	0,5539	0,7895	0,9998
M magenta red	0,3479	0,1423	0,6351	0,2595	0,9291
Y yellow	0,4424	0,5188	0,8110	0,9510	0,0711
D65 (white)	0,3333	0,3333	1,0000	1,0000	1,0000

E8581·

Figure 9: Data CIE *(x, y)* and *X, Y* and *Z* of complementary optimal colours with image technology normalization

Fig. 9 shows the CIE data *(x, y)* and *X, Y,* and *Z* now normalized between 0 and 1. This kind of normalisation is often used in image technology

> Remark: For the transfer of *X, Y,* and *Z* to *L*a*b** of CIELAB the same normalisation is used. *X, Y,* and *Z* is divided by X_n, Y_n, and Z_n (compare equations in Fig. 9 and Fig. 12).

As a result there is a normalisation of the CIE data *X, Y, Z* which gives tristimulus values X_{01}, Y_{01}, Z_{01} and $1–X_{01}$, $1–Y_{01}$, $1–Z_{01}$ for complementary optimal colours. A colour threshold formula needs to calculate the same threshold for both sets of data.

According to Fig. 9 the colour Violet blue V is the darkest colour (Y_{01}=0,0490) compared to White (Y_{01}=1,0000). For the optimal color Violet blue V the luminance ratio is 1 : 20 = 0,049 : 1,000. Among the six chromatic colours Yellow is the lightest one (Y_{01}=0,9509). For blue surface colours the *Y* value is usually less than half of the value Y_{01}=0,0490. This leads to a conflict with blue CIELAB data in vision. The luminance value of blue may be less compared to the luminance value of black which is Y_{01}=0,0400 for matt samples and Y_{01}=0,0250 for glossy samples. Some blue surface colours have Y_{01} values in this range and they still do not appear black and may be very chromatic.

The solution of the problem is the “chromatic strength” of the colour blue which is about 100 times larger compared to yellow. Chroma C^*_{ab} can be calculated by the product of *log* luminance and chromatic strength. Therefore

C^*_{ab} = chroma = *log* luminance x chromatic strength

So in principle the low luminance of blue may be compensated by the large chromatic strength of the blue.

3. CIELAB as basic for a new symmetric model of colour vision

A good first test of any new colour vision model is a study of the spacing in comparison with the *Munsell* and/or the *OSA* colour order system. CIELAB is based on the *Munsell* colour order system and there is a paper of Richter (1980) with colour figures of the samples of the *Munsell* and *OSA* colour order system in different chromaticity diagrams. This paper has the title “Cube root colour spaces and chromatic adaptation” Some of the following figures are from this paper.

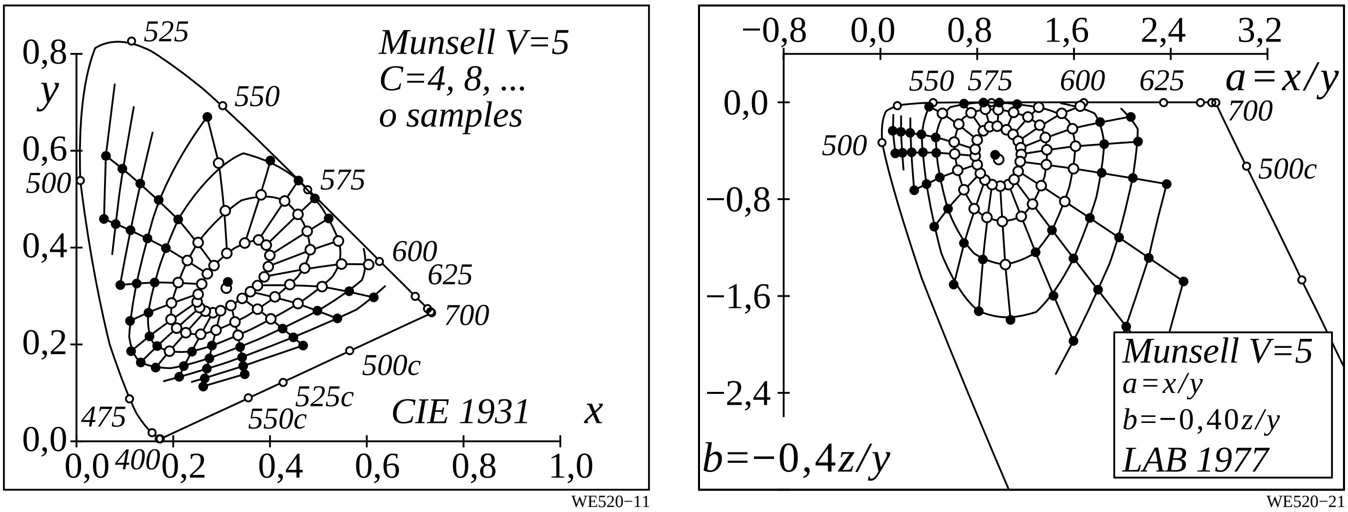

Figure 10: Real and extrapolated samples of the *Munsell* colour order system (Value 5) in *(x, y)* and *(a, b)*
Fig. 10 shows real (o) and extrapolated samples (•) of the *Munsell* colour order system for Value 5 in the CIE chromaticity diagram *(x, y)* and the chromaticity diagram *(a, b)*. The relation between the chromaticity coordinates *(a, b)* and *(x, y)* is given in Fig. 10 *(right)* and Fig. 11.

color valence metric (color data: linear relation to CIE 1931 data)		
linear color terms	**name and relationship to CIE tristimulues or chromaticity values**	**notes:**
luminous value	$Y = y\,(X + Y + Z)$	
chromatic value	*for linear chromatic value diagram (A, B)*	
red−green	$A = [X/Y - X_n/Y_n]\,Y = [a - a_n]\,Y$	*n=D65 (backgr.)*
	$= [x/y - x_n/y_n]\,Y$	
yellow−blue	$B = -0{,}4\,[Z/Y - Z_n/Y_n]\,Y = [b - b_n]\,Y$	
	$= -0{,}4\,[z/y - z_n/y_n]\,Y$	
radial	$C_{ab} = [A^2 + B^2]^{1/2}$	
chromaticity	*for (linear) chromaticity diagram (a, b)*	*compare to linear*
red−green	$a = X/Y = x/y$	*cone exitation*
yellow−blue	$b = -0{,}4\,[Z/Y] = -0{,}4\,[z/y]$	*P/ (P+D)*
radial	$c_{ab} = [(a - a_n)^2 + (b - b_n)^2]^{1/2}$	*T/ (P+D)*

VE780−7

Figure 11: Coordinates of the colour valence metric and the chromaticity coordinates *(a, b)*
Fig. 11 shows the coordinates of the colour valence metric with the chromaticity coordinates *(a, b)*. The chromatic values A and B can be calculated if for example the difference of the chromaticity *a* of the sample and the chromaticity a_n of the background (index n) is multiplied by the luminance factor *Y*. Additionally the chromaticity *a* and *b* are compared with the cone excitation *P / (P+D)* and *T / (P+D)*. At least the ratio *Z/Y = z/y* = [(1–*x*–*y*) / *y*] looks very similar compared to *T / (P+D)*. Later in this paper this relation will be discussed further.

Higher colormetric (color data: nonlinear relation to CIE 1931 data)		
non linear color terms	**name and relationship with tristimulues or chromaticity values**	**notes:**
lightness	$L^* = 116\ (Y/100)^{1/3} - 16\quad (Y > 0{,}8)$	*CIELAB 1976*
	Approximation: $L^* = 100\ (Y/100)^{1/2{,}4}$	
chroma	*non linear transform of chromatic values A and B*	
red−green	$a^* = 500\ [\ (X/X_n)^{1/3} - (Y/Y_n)^{1/3}\ ]$	*CIELAB 1976*
	$= 500\ (a' - a'_n)\ Y^{1/3}$	*n=D65 (backgr.)*
yellow−blue	$b^* = 200\ [\ (Y/Y_n)^{1/3} - (Z/Z_n)^{1/3}\ ]$	*CIELAB 1976]*
	$= 500\ (b' - b'_n)\ Y^{1/3}$	
radial	$C^*_{ab} = [\ a^{*2} + b^{*2}\ ]^{1/2}$	
exitation ?	*nonlinear transform of chromaticities a=x/y and b=z/y*	
red−green	$a' = (1/X_n)^{1/3}\ (x/y)^{1/3}$	*compare to log*
	$= 0{,}2191\ (x/y)^{1/3}$ for *D65*	*cone exitation*
yellow−blue	$b' = -0{,}4\ (1/Z_n)^{1/3}\ (z/y)^{1/3}$	***log[P/(P+D)]***
	$= -0{,}08376\ (z/y)^{1/3}$ for *D65*	***log[T/(P+D)]***
radial	$c'_{ab} = [\ (a' - a'_n)^2 + (b' - b'_n)^2\ ]^{1/2}$	

VE781−7

Figure 12: Coordinates of the higher colour metric with the non linear chromaticity coordinates *(a', b')*

Fig. 12 shows the coordinates of the higher colour metric with the non linear chromaticity coordinates *(a', b')*. The CIELAB chroma data a^* and b^* can be calculated if for example the difference of the non linear chromaticity a' of the sample and the non linear chromaticity a'_n of the background is multiplied by the lightness L^*. Additionally the non linear chromaticity a' and b' are compared with the cone excitation log [*P / (P+D)*] and log [*T / (P+D)*]. At least the cube root ratio $(Z/Y)^{1/3} = (z/y)^{1/3} = [\ (1–x–y)\ /\ y\ ]^{1/3}$ looks very similar to log [*T / (P+D)*]. Later in this paper these relations will be discussed further.

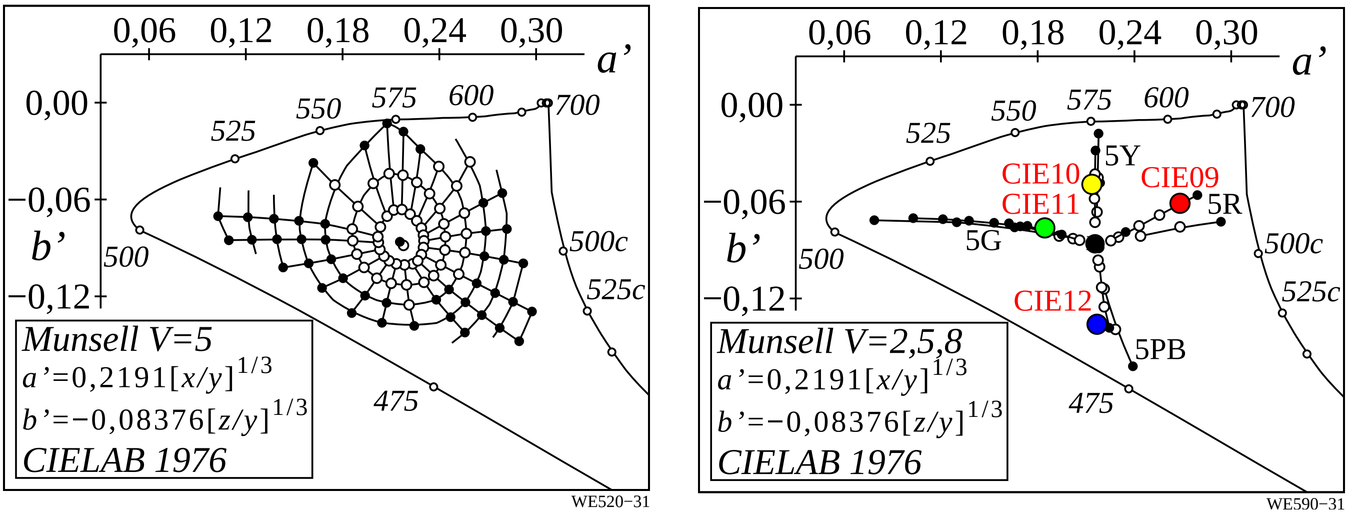

Figure 13: Real and extrapolated samples of the *Munsell* colour order system (Value 5) in *(a', b')*

Fig. 13 shows real (o) and extrapolated samples (•) of the *Munsell* colour order system for Value 5 in the non linear chromaticity diagram *(a', b') (left)* and the elementary hues *5R, 5Y, 5G* and *5PB* of the *Munsell* colour order system for *Value* 2, 5, and 8 in the non linear chromaticity diagram *(a', b')*. Additionally the four CIE-test colours no. 9 to 12 of CIE 13.3 are plotted. These four colours serve as elementary colours in the field of image technology. The spectral data of these colours are defined and they serve for example in ISO/IEC 15775 as reference colour for colour copiers.

The elementary colours Yellow *J* and Blue *B* are approximately on a line through the white point (chromaticity of D65). The elementary colours Red *R* and Green *G* are not on a line through the white point. For D65 the hue angles h_{ab} are 26, 92, 162 and 272 in the CIELAB system for the four elementary colours *RJGB*.

A colour vision model shall describe the elementary colours and approximately the location on these hue angles.

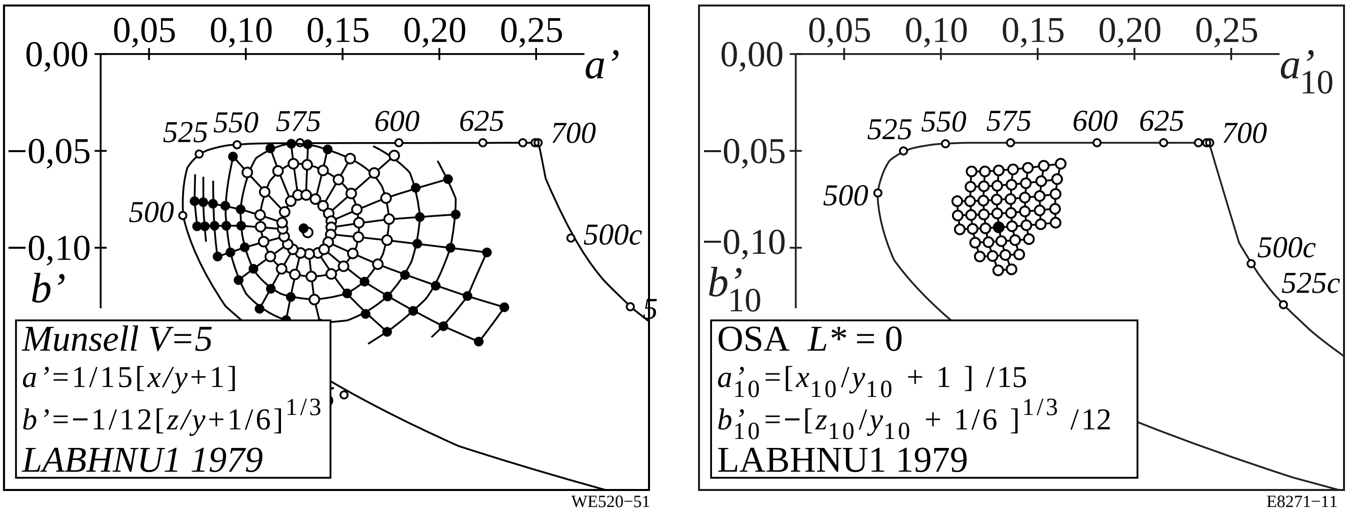

Figure 14: Samples of the *Munsell* and *OSA* colour order system in a modified *(a', b')* diagram

Fig. 14 shows the samples (Value 5) of the *Munsell* colour order system and the samples (*L*=0) of the *OSA* colour order system in a modified non linear chromaticity diagram *(a', b')*. The relation of *(a', b')* and *(x, y)* is given in the figure. According to the results of the output spacing it is possible to use a linear equation in red–green direction.

A colour vision model shall explain and use this linear property in red–green direction and the non linear property in yellow–blue direction.

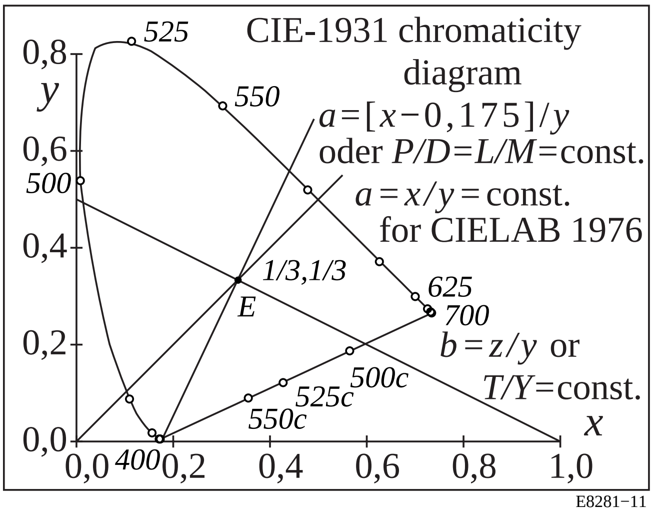

Figure 15: Axis of excitation *P/D* and *T/Y* and chromaticity *(a, b)* in the CIE chromaticity diagram *(x, y)*

Fig. 15 shows the axis of excitation *P/D* and *T/Y* and the chromaticity *(a, b)* in the CIE chromaticity diagram *(x, y).* The *a* coordinate used for the transformation in CIELAB is different compared to the axis *a* = [*x* –0,175] / *y* which is defined by the constant ratio *P/D*. The *b*-axis is identical to the axis defined by the constant ratio *T/Y.* The remaining axis *T/P* and *T/D* are not plotted.

In the following different basic properties of the colour valence and the higher colour metric are shown. The higher colour metric is represented by CIELAB and this metric is used to create a symmetric colour vision model for static stimuli. One can assume either adjacent or separated stimuli in a grey background which are viewed with a white border. For this model we can assume the chromaticity of D65 for both the grey background and the white border. The luminance of the white border or the white screen in the office shall be approximately 500 cd/m^2 for this model. Then the grey luminance is 100 cd/m^2 if the luminance reflectance is *Y* = 20 for the grey monitor background.

4. Mean sensitivity and chromatic adaptation of the three cones

The three cone sensitivities $P_o(\lambda)$, $D_o(\lambda)$ and $T_o(\lambda)$ are usually normalized to one at the maximum in a linear plot which corresponds to zero in a logarithmic plot. This normalization is indicated by an index o in this paper.

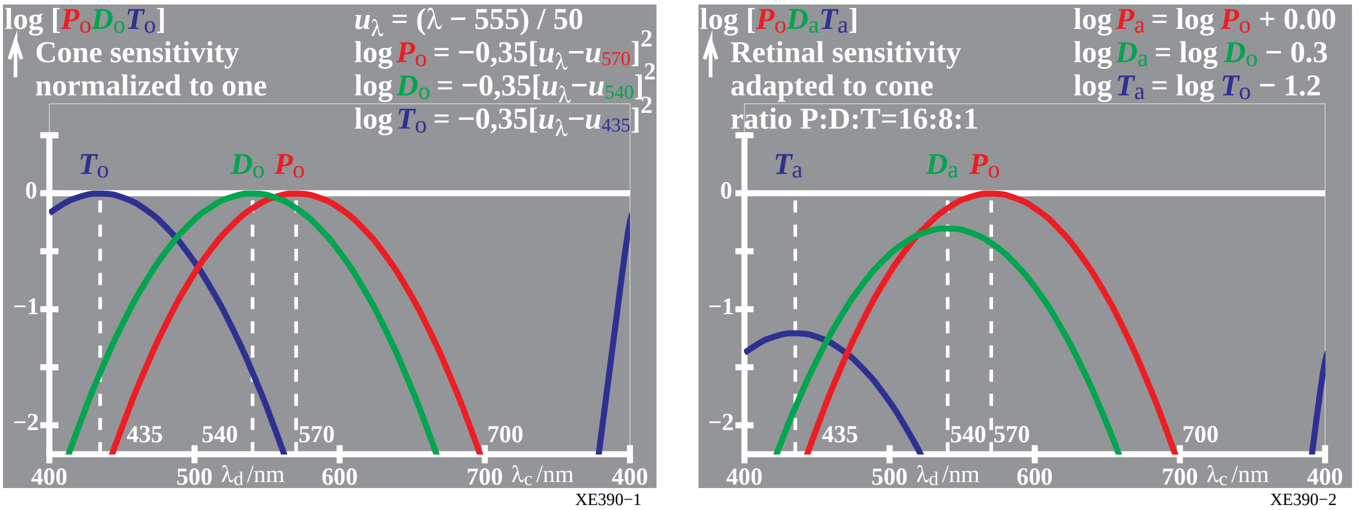

Figure 16: Normalized sensitivity of three cones and the retina sensitivity for the cone ratio *P:D:T* = 16:8:1

Fig. 16 shows the normalized sensitivity of the three cones and the retina sensitivity for the cone ratio *P:D:T* = 16:8:1. This cone ratio varies across the retina and the used ratio is a good representation for the fovea.

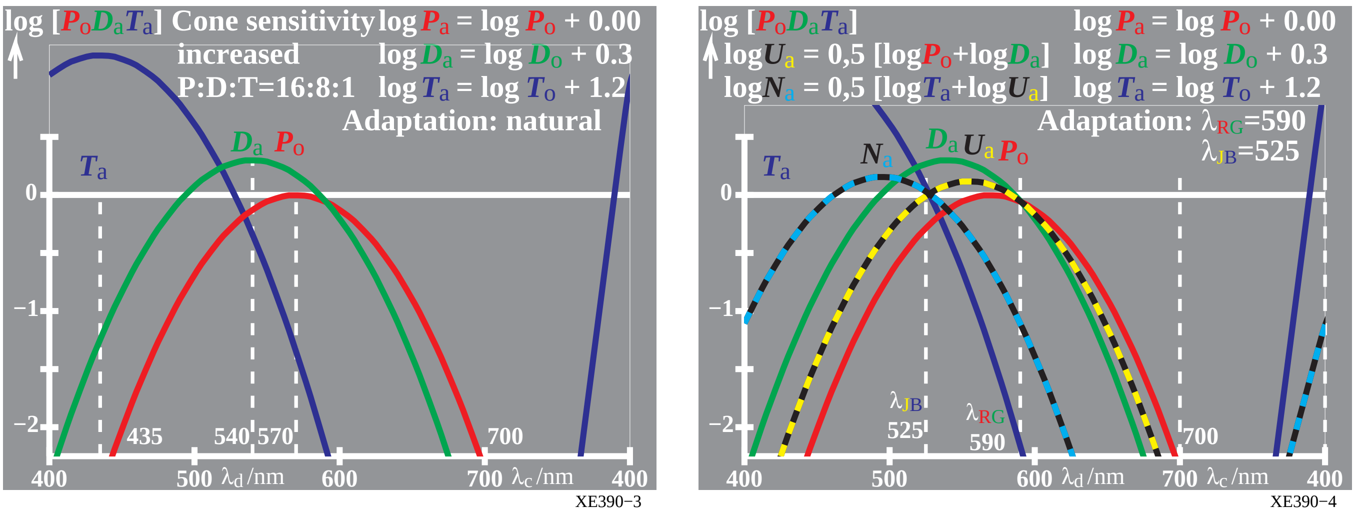

Figure 17: Adapted cone sensitivities for the retina cone ratio *P:D:T* = 16:8:1 and the sensitivities U_a and N_a

Fig. 17 shows the adapted cone sensitivities for the retina cone ratio *P:D:T* = 16:8:1 and the calculated “sensitivities” U_a and N_a *(right).* If all sensitivities are normalized to 1 in a linear and to 0 in a logarithmic plot, compare Fig. 1, then the maximum and shape of the sensitivities $U_a(\lambda)$ and $N_a(\lambda)$ are very similar compared to the photopic sensitivity $V(\lambda)$ and the scotopic sensitivity $V'(\lambda)$. We conclude:

1. The sensitivity $U_a(\lambda)$ has the maximum at 555nm which is in the middle between 540 and 570nm. This sensitivity is similar to the CIE photopic sensitivity $V(\lambda)$.
2. The sensitivity $N_a(\lambda)$ has the maximum at 495nm which is in the middle between 435 and 555nm. This sensitivity is similar to the CIE scotopic sensitivity $V'(\lambda)$.
3. The absolute values of the maxima of $U_a(\lambda)$ and $N_a(\lambda)$ are approximately the same in Fig. 17 *(right).*

Remark: If instead of the maximum 435nm the maximum 445nm is used for the blue cone T which is in better agreement with CIE 170-1:2006 then the sensitivity $N_a(\lambda)$ has the maximum at 500nm. This is in better agreement with the maximum of the CIE scotopic sensitivity $V'(\lambda)$. As indicated earlier we use 435nm here for a better agreement of experimental results in the wavelength range larger 435nm, compare Fig. 1. If the sensitivities are calculated as function of frequency and in quantum units this difficulty disappears to a high degree, compare Richter (1996). At present the colorimetry according to CIE 15:2004 is based on the wavelength scale and the spectral radiance. Therefore is seems more appropriate to choose the wavelength scale and radiance units instead of the frequency scale and quantum units.

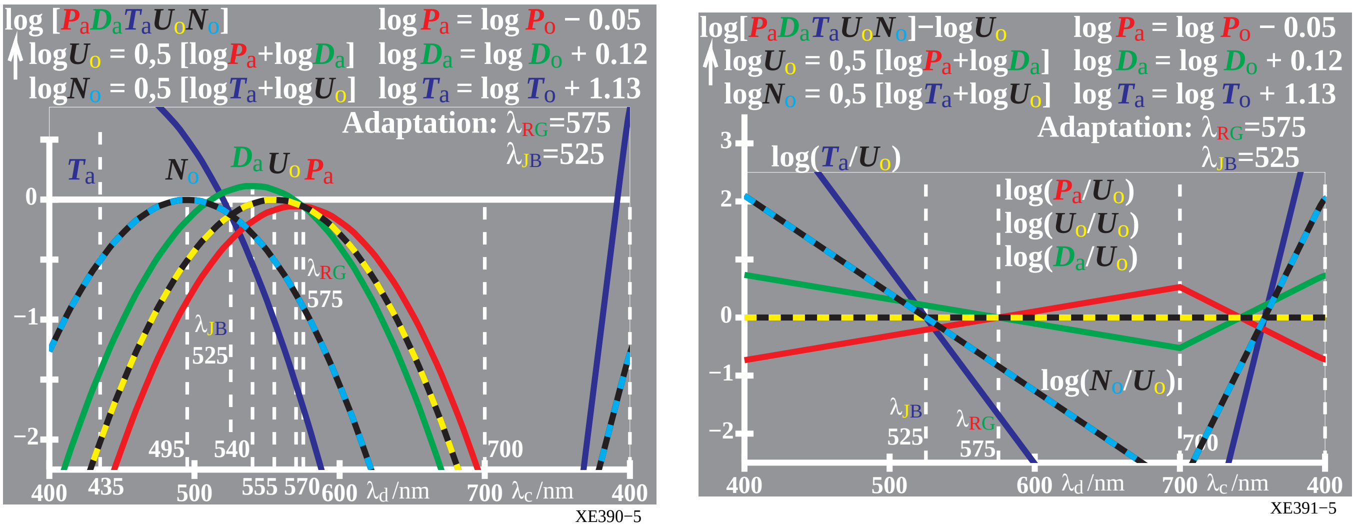

Figure 18: Normalized sensitivities U_o and N_o and sensitivities P_a, D_a, T_a *(left)* and excitation e_{xU} *(right)*

Fig. 18 shows the normalized sensitivities U_o and N_o and the sensitivities P_a, D_a, T_a *(left)* and the excitations e_{xU} *(right)*. The indices xU correspond to the sensitivity difference of $x = (P, D, T)$ and U.

In Fig. 18 the value of both maxima is normalized to one (linear) and zero (logarithmic). This property produces a symmetry compared to the wavelength 525nm. The following equations for the sensitivities are valid

$\log U_o(\lambda) = 0{,}5\,[\log P_a(\lambda) + \log D_a(\lambda)]$

$\log N_o(\lambda) = 0{,}5\,[\log T_a(\lambda) + \log U_o(\lambda)]$

and the following equations for the excitations $e_{xU}(\lambda)$, $(x = P, D)$ and $e_{xN}(\lambda)$, $(x = T, U)$

$e_{PU}(\lambda) = \log [P_a(\lambda) / U_o(\lambda)] = \log P_a(\lambda) - \log U_o(\lambda)$

$e_{DU}(\lambda) = \log [D_a(\lambda) / U_o(\lambda)] = \log D_a(\lambda) - \log U_o(\lambda)$

$e_{TN}(\lambda) = \log [T_a(\lambda) / N_o(\lambda)] = \log T_a(\lambda) - \log N_o(\lambda)$

$e_{UN}(\lambda) = \log [U_o(\lambda) / N_o(\lambda)] = \log U_o(\lambda) - \log N_o(\lambda)$

The excitations in photopic units *(U)* and scotopic units *(N)* are straight lines. The cut points are at 575nm for the red–green adaptation and at 525nm for the yellow–blue adaptation. If for example the red–green adaptation is changed to 525nm then the excitation $\log [P_a(\lambda) / U_o(\lambda)]$ cuts the yellow–black zero line at 525nm. The equation

$\log U_o(\lambda) = 0{,}5\,[\log P_a(\lambda) + \log D_a(\lambda)]$

is valid for **any** red–green adaptation condition.

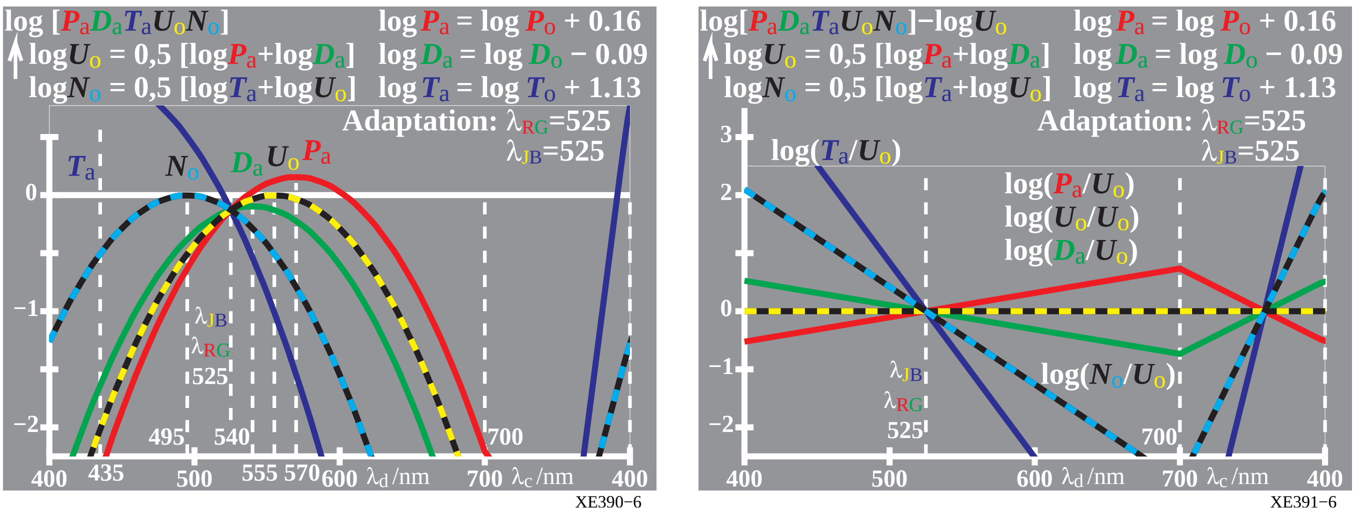

Figure 19: Sensitivities U_o, N_o, P_a, D_a, T_a *(left)* and the excitation e_{xU} *(right)* for the RG-adaptation to 525nm

Fig. 19 shows the sensitivities U_o, N_o, P_a, D_a, T_a *(left)* and the excitation e_{xU} *(right)* for red–green (RG-)adaptation to

525nm. The following equations for the excitations $e_{xU}(\lambda)$ are valid:

$e_{PU}(\lambda) = \log [\, P_a(\lambda) \,/\, U_o(\lambda) \,]$

$e_{DU}(\lambda) = \log [\, D_a(\lambda) \,/\, U_o(\lambda) \,]$

$e_{TU}(\lambda) = \log [\, T_a(\lambda) \,/\, U_o(\lambda) \,]$

$e_{NU}(\lambda) = \log [\, N_o(\lambda) \,/\, U_o(\lambda) \,]$

The plot on the right side shows very unique properties:

1. All four excitations cut at 525nm
2. The slope is largest for $e_{TU}(\lambda)$ and about 2 per 100nm.
3. The slope of $e_{NU}(\lambda)$ *is 1/2 compared to the slope of* $e_{TU}(\lambda)$.
4. The slope of $e_{PU}(\lambda)$ *is 1/8 compared to the slope of* $e_{TU}(\lambda)$

The factors 1/2 (=60/120) and 1/8 (=15/120) are only determined by the wavelength difference of the maxima of the different sensitivities compared to the maximum of $U_o(\lambda)$. The wavelength difference is

120nm (= |435nm – 555nm|) between $T_o(\lambda)$ and $U_o(\lambda)$

60nm (= |495nm – 555nm|) between $N_o(\lambda)$ and $U_o(\lambda)$

15nm (= |540nm – 555nm| = |570nm – 555nm|) between $D_o(\lambda)$ and $U_o(\lambda)$ *or* $P_o(\lambda)$ and $U_o(\lambda)$

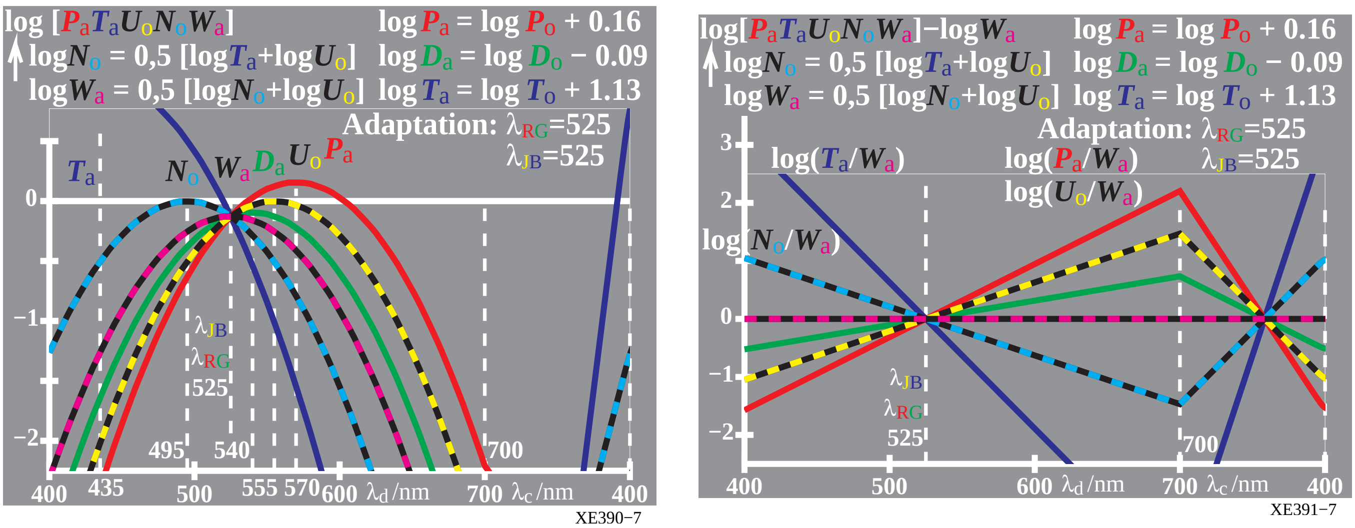

Figure 20: Sensitivities U_o, N_o, W_a, P_a, D_a, T_a *(left)* and excitations e_{xW} *(right)* for the RG-adaptation to 525nm

Fig. 20 shows the sensitivities U_o, N_o, W_a, P_a, D_a, T_a *(left)* and excitations e_{xW} *(right)* for red–green (RG-) adaptation to 525nm. The following additional equations define the "mesopic" sensitivity $W_a(\lambda)$ as mean of the "photopic" sensitivity $U_o(\lambda)$ and the "scotopic" sensitivity $N_o(\lambda)$

$\log W_a(\lambda) = 0{,}5\, [\, \log N_o(\lambda) + \log U_o(\lambda) \,]$

The following equations for the "mesopic" excitations $e_{xW}(\lambda)$:

$e_{PW}(\lambda) = \log [\, P_a(\lambda) \,/\, W_a(\lambda) \,]$

$e_{DW}(\lambda) = \log [\, D_a(\lambda) \,/\, W_a(\lambda) \,]$

$e_{TW}(\lambda) = \log [\, T_a(\lambda) \,/\, W_a(\lambda) \,]$

$e_{UW}(\lambda) = \log [\, U_o(\lambda) \,/\, W_a(\lambda) \,]$

$e_{NW}(\lambda) = \log [\, N_o(\lambda) \,/\, W_a(\lambda) \,]$

are a further step to more symmetry:

1. the slope of $\log [\, U_o(\lambda) \,/\, W_a(\lambda) \,]$ is equal to the negative slope of $\log [\, N_o(\lambda) \,/\, W_a(\lambda) \,]$.
2. the slope of $\log [\, N_o(\lambda) \,/\, W_a(\lambda) \,]$ is 1/3 compared to the slope of $\log [\, T_a(\lambda) \,/\, W_a(\lambda) \,]$.

Additionally we recognize that:

3. the slope of $\log [\, N_o(\lambda) \,/\, U_o(\lambda) \,]$ is 1/2 compared to the slope of $\log [\, T_a(\lambda) \,/\, U_o(\lambda) \,]$.
4. the slope of $\log [\, W_a(\lambda) \,/\, U_a(\lambda) \,]$ is 1/2 compared to the slope of $\log [\, N_o(\lambda) \,/\, U_a(\lambda) \,]$.

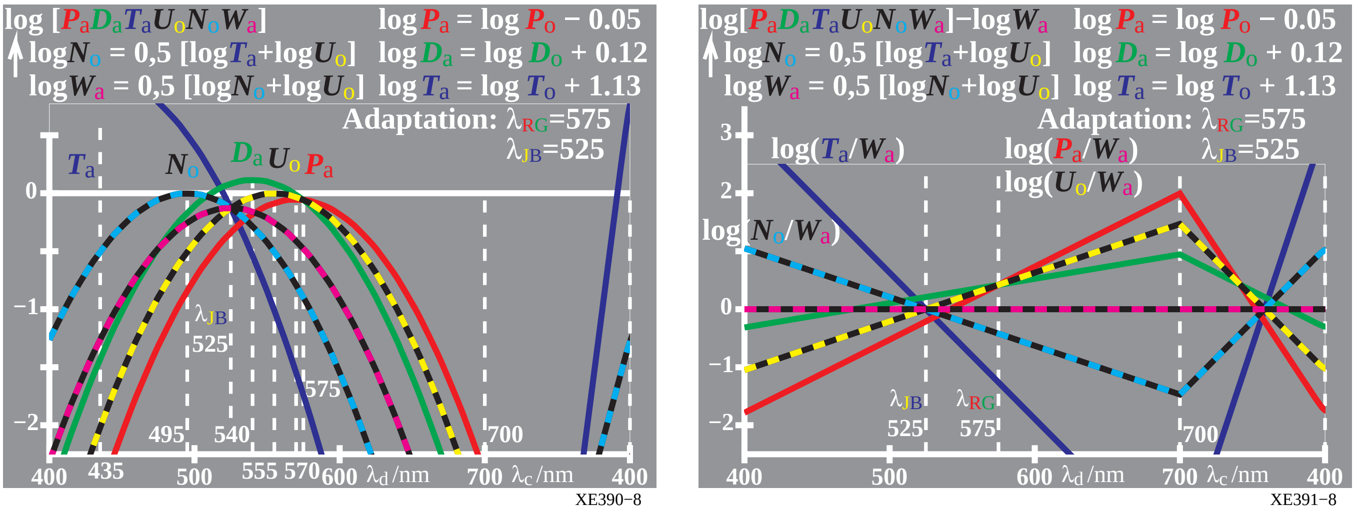

Figure 21: Sensitivities U_o, N_o, W_a, P_a, D_a, T_a *(left)* and excitations e_{xW} *(right)* for the RG-adaptation to 575nm

Fig. 21 shows the sensitivities U_o, N_o, W_a, P_a, D_a, T_a *(left)* and excitations e_{xW} *(right)* for red–green (RG-) adaptation to 575nm. There is a RG-adaptation change from 525nm to 575nm between Fig. 20 and 21. The elementary colour Yellow *J* has in white backgrounds the dominant wavelength λ_d = 575nm. There is the wish to describe this property and therefore this change is necessary. One must realize that a change of $U_o(\lambda)$ is not necessary for this change of RG-adaptation. Only the weighting of $P_a(\lambda)$ and $D_a(\lambda)$ changes according to the equation

$$\log U_o(\lambda) = 0{,}5\,[\,\log P_a(\lambda) + \log D_a(\lambda)\,]$$

According to Fig. 20 for *RG*-adaptation to 525nm it is valid:

$$\log P_a(\lambda) = \log P_o(\lambda) + 0{,}16$$

$$\log D_a(\lambda) = \log D_o(\lambda) - 0{,}09$$

and according to Fig. 21 for *RG*-adaptation to 575nm it is valid:

$$\log P_a(\lambda) = \log P_o(\lambda) - 0{,}05$$

$$\log D_a(\lambda) = \log D_o(\lambda) + 0{,}12$$

Dependent on the *RG*-adaptation wavelength (λ_{RG} >= 525 nm) the following equations allow to determine the constants in the above equations. For any *RG*-adaptation the excitations $e_{PU}(\lambda_{RG})$ and $e_{DU}(\lambda_{RG})$ are equal:

$$e_{PU}(\lambda_{RG}) = e_{DU}(\lambda_{RG})$$

or

$$\log\,[\,P_a(\lambda_{RG})\,/\,U_o(\lambda_{RG})\,] = \log\,[\,D_a(\lambda_{RG})\,/\,U_o(\lambda_{RG})\,]$$

or

$$\log P_a(\lambda_{RG}) = \log D_a(\lambda_{RG})$$

or

$$\log P_o(\lambda_{RG}) + a_P = \log D_o(\lambda_{RG}) + a_D$$

Together with

$$\log U_o(\lambda_{RG}) = 0{,}5\,[\,\log P_a(\lambda_{RG}) + \log D_a(\lambda_{RG})\,]$$

which leads to

$$\log U_o(\lambda_{RG}) = 0{,}5\,[\,\log P_o(\lambda_{RG}) + a_P + \log D_o(\lambda_{RG}) + a_D\,] = 0{,}5\,[\,2\,\{\,\log P_o(\lambda_{RG}) + a_P\,\}\,] = \log P_o(\lambda_{RG}) + a_P$$

or

$$a_P = -\,[\,\log P_o(\lambda_{RG}) - \log U_o(\lambda_{RG})\,]$$

$$= -\log\,[\,P_o(\lambda_{RG})\,/\,U_o(\lambda_{RG})\,] = -\,e_{PU}(\lambda_{RG})$$

$$a_D = -\,[\,\log D_o(\lambda_{RG}) - \log U_o(\lambda_{RG})\,]$$

$$= -\log\,[\,D_o(\lambda_{RG})\,/\,U_o(\lambda_{RG})\,] = -\,e_{DU}(\lambda_{RG})$$

Therefore chromatic *RG*-adaptation to any wavelength λ_{RG} is only a shift by a constant defined by the excitations $e_{PU}(\lambda_{RG})$ or $e_{DU}(\lambda_{RG})$.

5. Impulse rate in the retina as function of relative luminance

5.1 Impulse rates and changes for achromatic colours

Richter (1996) has shown in a book the different sensitivities and excitations (called *saturations*) which are calculated as function of wavelength with the CIE colour matching functions or the CIE chromaticity [$x(\lambda)$, $y(\lambda)$]. He also showed the different achromatic and chromatic signals as function of luminance L or relative luminance $L_r = L / L_b$ (b = background).

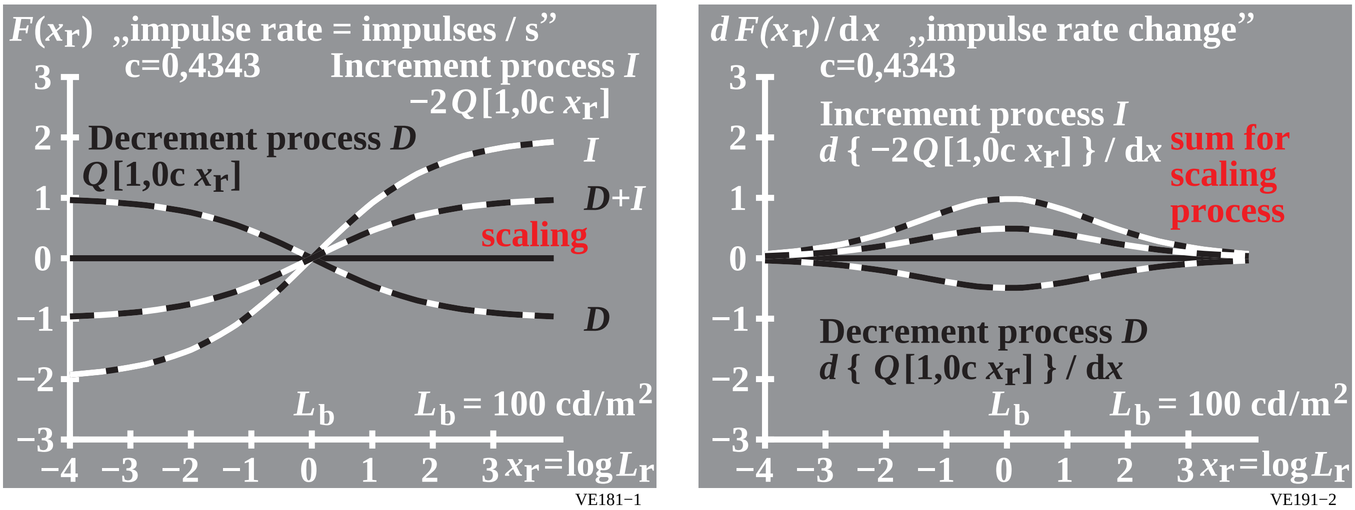

Figure 22: Three visual processes as function of luminance: Increment *(I)*, Decrement *(D)* and the sum *(D+I)*

Fig. 22 shows three visual processes as function of luminance: Increment *(I)*, Decrement *(D)* and the sum *(D+I)*. The signals (Impulses/sec in the retina) of the *I*-process increase with luminance, the signals of the *D*-process decrease with luminance and the signals of the *D+I*-process increase. Richter (1996) has called the *D*-process the black-process *N* because there are larger responses for the blackish colours (N = french noir = black) compared to the grey background. The *I*-process was called the white process *W* because there are larger responses for the whitish colours compared to the grey background. Instead of *N, W* and *N+W* we use in the following the abbreviations *D, I* and *D+I*. This is the more modern terminology which is used in the book of *Valberg* (2005).

In Fig. 22 *(right)* the "impulse rate changes" are shown as function of relative luminance. The largest change is for the *I*-process at the relative luminance $L_r = 1$ which is at the grey background luminance L_b =100 cd/m^2. Both for the *D*-process and the *D+I*-process the absolute value of the change is about half compared to the *I*-process.

5.2 Impulse rate in the retina and changes for chromatic colours

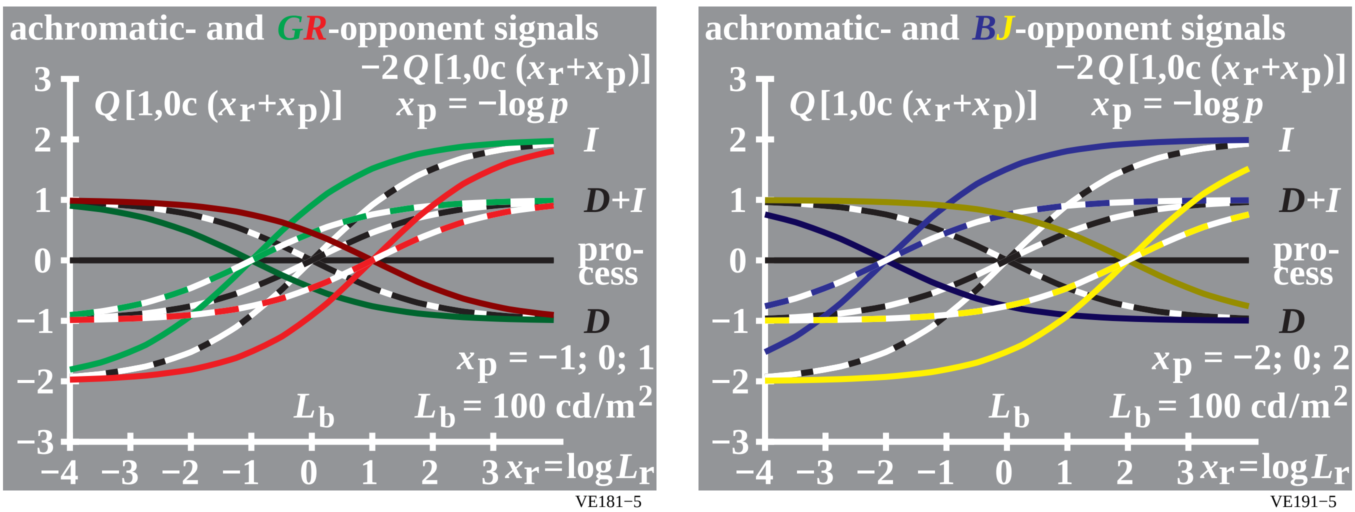

Figure 23: Nine visual processes as function of luminance for achromatic and chromatic colours.

Fig. 23 shows nine visual processes as function of luminance for achromatic and chromatic colours. Therefore we have three times the number of processes compared to the achromatic colours.

Richter (1996) has developed a function ***Q*** and has shown that the parameters of the function Q depend on relative luminance L_r and purity p. The negative logarithmic purities p ($x_p = -\log p$) in green–red and blue–yellow direction seem to be in a first approximation the excitations e_{PU} and e_{TU}. Therefore we can write

$x_r = \log [\, L / L_b \,] = \log L_r$

$x_{pGR} = e_{PU} = \log [\, P_a / U_o \,]$

$x_{pBJ} = e_{TU} = \log [\, T_a / U_o \,]$

In Fig. 23 for the excitation in green–red direction the three values $x_{pGR} = e_{PU} = -1$, 0 and 1 are used *(left)* and for the excitation in blue–yellow direction the three values $x_{pBJ} = e_{TU} = -2$, 0 and 2 are used *(right)*. These numbers are realistic numbers for the different visual *GR*- and *BJ*-processes. In the retina addtionally to theprocesses *GR* and *BJ* there are the complementary processes *RG* and *JB* which are not shown here.

5.3 Vision and cone excitation and delete of the lighter opponent process

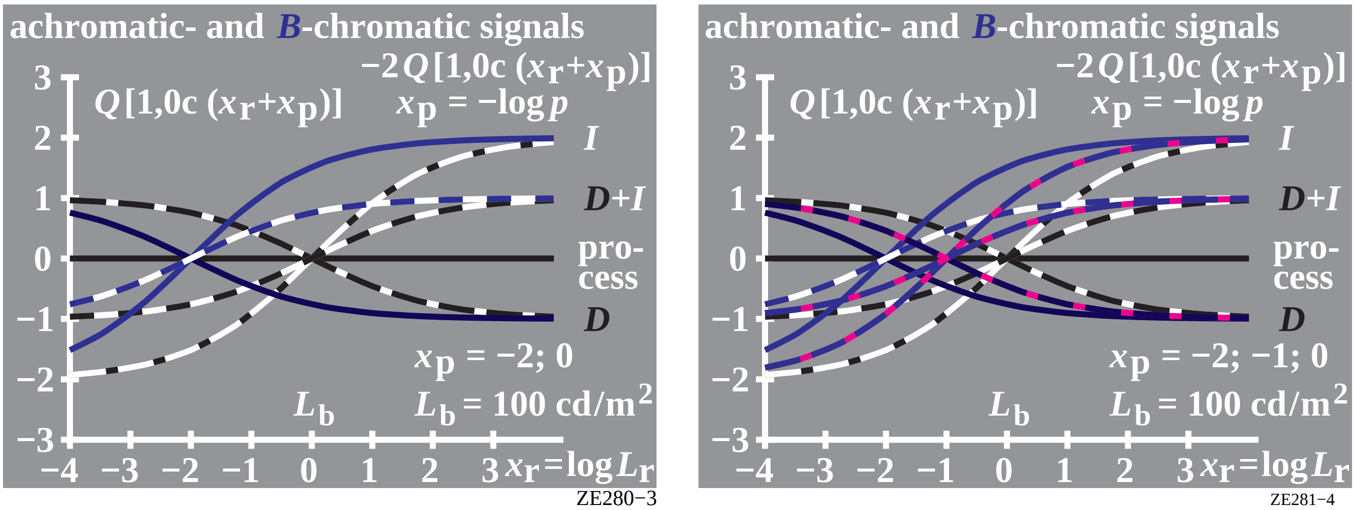

Figure 24: Six *(left)* and nine *(right)* visual processes as function of luminance for achromatic and blue colours

Fig. 24 shows six *(left)* and nine *(right)* visual processes as function of luminance for achromatic and blue colours. The light and complementary yellow components of Fig. 23 are deleted in Fig. 24.

It seems an important strategy of the visual human system to use only the blue components of the *BJ*-process (and the yellow component of the *JB*-process and similar for the *RG*- and *GR*-process). We know from Fig. 8 that the optimal colour Violet blue V has only the luminance factor 4,9 compared to 100 for white. Many real blue colours may have only half of this value. Therefore it is important for the visual system to produce a large chroma signal for a blue colour especially because for blue colours the luminance factor is often by a factor 40 less compared to white.

In Fig. 24 the excitation of the blue process has the value 2 which produces a shift of two log luminance units (1/100) towards lower luminance on the luminance scale. Therefore in Fig. 24 for the luminance which is 100 times less compared to the background luminance there is the largest luminance change of the blue monochromatic wavelength $\lambda_B = 475$ nm.

If the difference between the two *I*-processes *blue* and *achromatic* is calculated, then the largest difference is only one (and not two) log luminance units below the background luminance. If this is called the chromatic signal then the maximum chromatic signal is one log unit below the background luminance. This is different compared to the two log units for the maximum slope change for luminance. It remains the question at which luminance the largest change of the chromatic signal occurs.

Richter (2006b) has produced a model for the threshold and scaling of only achromatic colours. For adjacent colours the difference of the colour signals plays the main role but for separated colours the mean log value of the sample and the background has to be calculated first to describe the experimental results.

Therefore in Fig. 24 *(right)* the mean of the two *I*-processes blue and achromatic is calculated (in red-blue colour). It is obvious that the mean process and all others between the blue and the achromatic process shift only one unit below the background luminance. So in this case a blue colour of the monochromatic wavelength $\lambda_B = 475$nm in a grey background has the maximum change of the chromatic signal one unit below the grey background luminance. If the luminance factor is Y = 20 for the background then for blue the chromatic signal is largest, if the luminance factor is about Y = 2.

For most of the people who work with colorimetry this seems unpossible compared to experience. For many years they know that for example the black N of offset colour printing has the luminance factor Y = 2,5. The value Y = 2 of blue is below and therefore the statement is: the monochromatic colour λ_B = 475 nm with Y = 2 must appear black.

But there is a strong argument against. A monochromatic stimuli of λ_B = 475 nm with Y = 2 is not among the real surface colours. So a proof is only possible with special coloured lights in a laboratory. Many of such experiments produced with colour filters and projectors are described in a book of *Evans* (1974).

5.4 Maximum luminance discrimination, chromatic and chroma signal

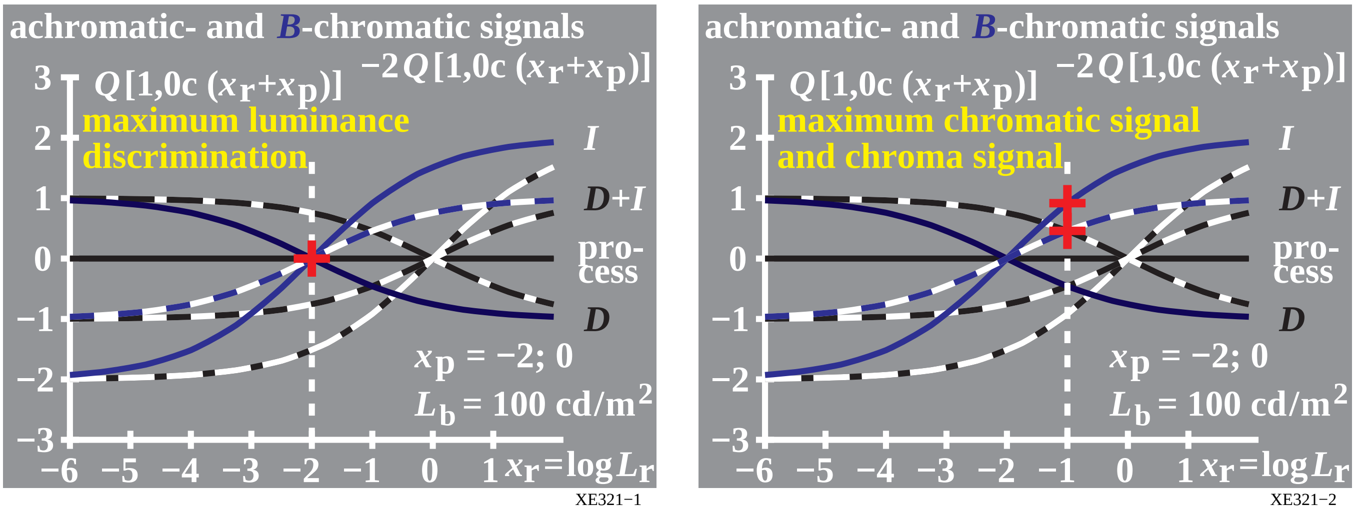

Figure 25: Maximum luminance discrimination, chromatic and chroma signal

Fig. 25 shows the maximum luminance discrimination *(left)* and the maximum chromatic and chroma signals *(right)*. The slopes for luminance discrimination of the *I*-process and the *D+I*-process are largest *(left)* at the red mark. This is two log units below the background luminance. The chromatic signal is largest for the *I*-process at one red mark *(right)* and the chroma signal is largest for the *D+I*-process at the other red mark *(right)*. both marks are one log unit below the background luminance.

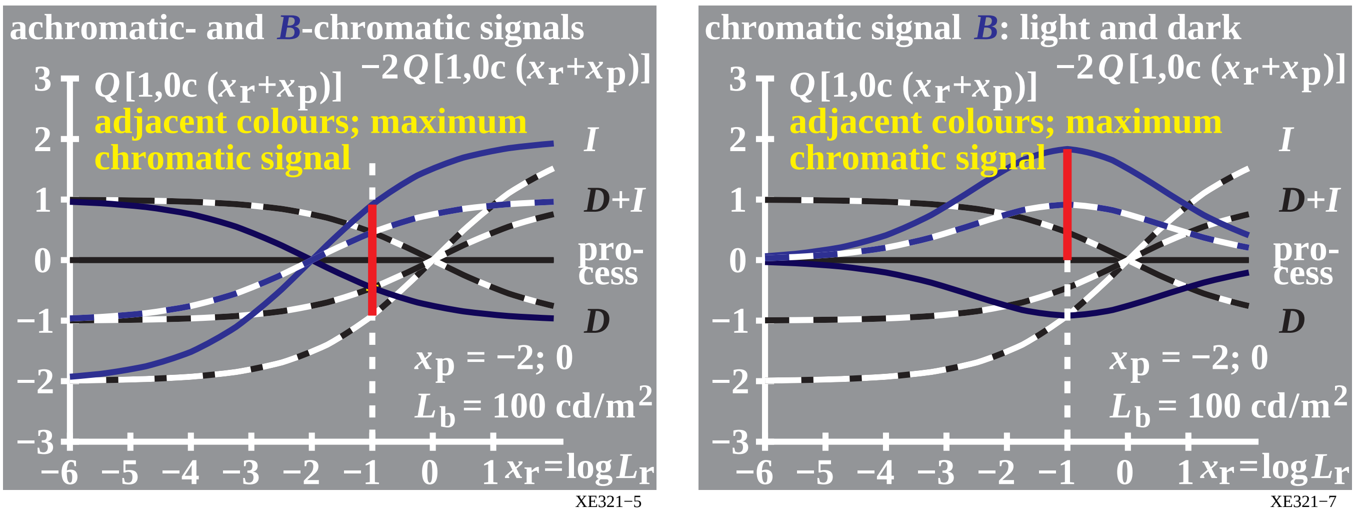

Figure 26: Chromatic signals as function of relative luminance L_r

Fig. 26 shows a red line for the chromatic signal *(left)*. The chromatic signals are calculated and plotted as function of luminance *(right)*. The maximum chromatic signal is one log unit below the background luminance.

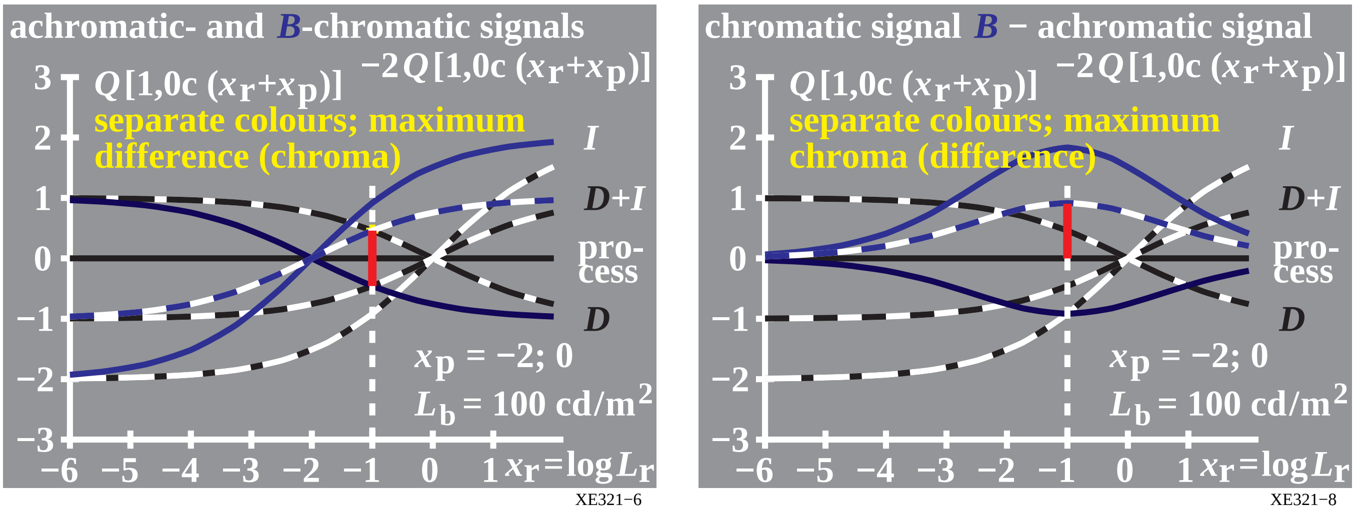

Figure 27: Chroma signals as function of relative luminance L_r

Fig. 27 shows a red square for the chroma signal *(left)*. The chroma signals are shown as function of relative luminance *(right)*. The maximum chromatic signal is one log unit below the background luminance.

The difference between the chromatic and chroma signal has to be clarified further in experiments. It is likely that there is a connection with the two viewing conditions of adjacent and separated colours in a grey background. In a first approximation the colour difference of adjacent colours depends not much on the background. However, the colour difference of separated colours (separated colour order samples on a grey background) depends very much on the background. This seem to be the reason, that the chroma signal depends on the mean logarithmic signal of the sample and background. The chromatic signal depends only on the mean log signal of the two adjacent samples. The mean signal of the two adjacent samples is for small colour differences not very different compared to one of the sample signals. Therefore the difference between the chromatic and the chroma signal increases with increasing difference of the sample and the background.

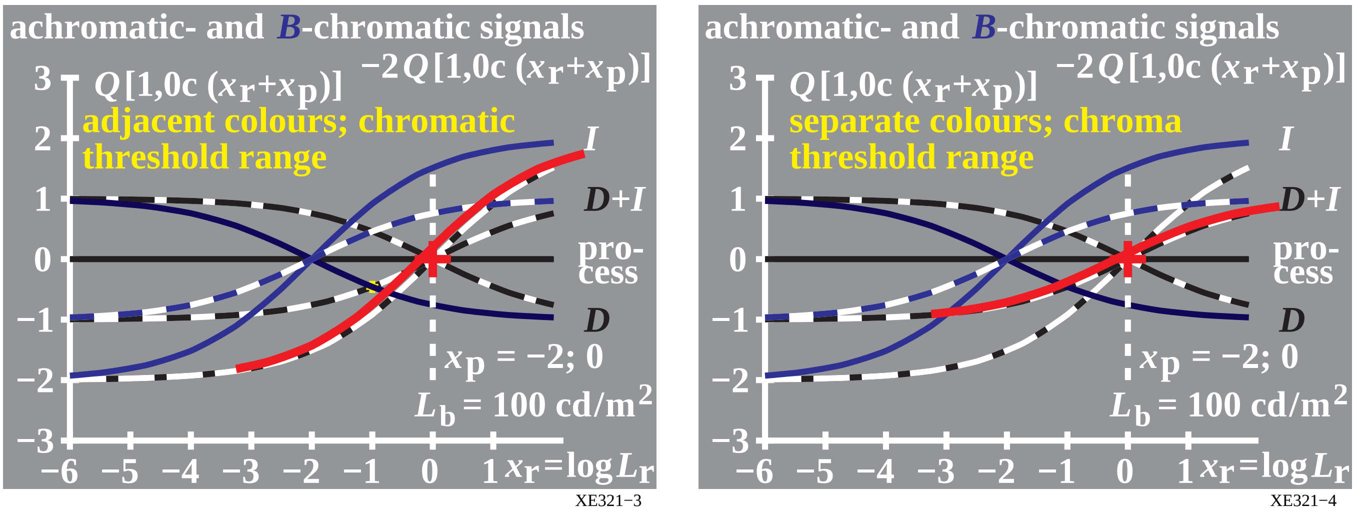

Figure 28: Chromatic and chroma threshold for nearly achromatic colors at different luminance

Fig. 28 shows the chromatic and chroma threshold for nearly achromatic colors at different luminance. The two red *S*-shaped curves follow the achromatic *I*-process *(left)* and the achromatic *D+I*-process *(right)* along the luminance axis. The slopes are 1,0 and 0,5 at the background luminance.

In terms of CIE colorimetry for monochromatic colours of equal luminance there is a definite purity for each wavelength at which a characteristic hue appears. This is the **chromatic threshold**. For the *I*-process and the *D+I*-process therefore we can expect some shift along the x_r-axis compared to the achromatic signals.

It seems surprising that this shift is small and **constant** on the luminance scale for all stimuli between the chromatic threshold for very dark colours up to the grey background and above to the white border colour.

There are different methods in vision to determine this threshold by the following experimental conditions:

1. one can add monochromatic light to a grey uniform background until a hue appears.
2. one can add monochromatic light to a black circular center field in a grey background until a hue appears
3. one can add monochromatic light to a black circular center field for only one half of the circular center field in a grey background until a hue appears
4. In case of 2 or 3 if a hue has appeared one can add achromatic light of the background chromaticity until the grey background luminance is reached and further until the luminance of the white border is reached and above.

Evans (1974) reported in his book in a section “chromatic threshold” on page 113;

> “We discovered the surprising fact that if this monochromatic luminance (the chromatic threshold luminance of the above case 2 near black) was left constant and white light was added, the mixture **remained at the chromatic threshold all the way up to a luminance match with the white background**”

Therefore at least in case 2 there is only a constant shift for the chromatic threshold along the x_r-axis. Case 2 is the chroma situation and this is shown in Fig. 28 *(right)*. Experimental results according to case 3 are not known and any set of experimental data is appreciated.

6. Elementary colours

6.1 Experimental models and data for elementary colours

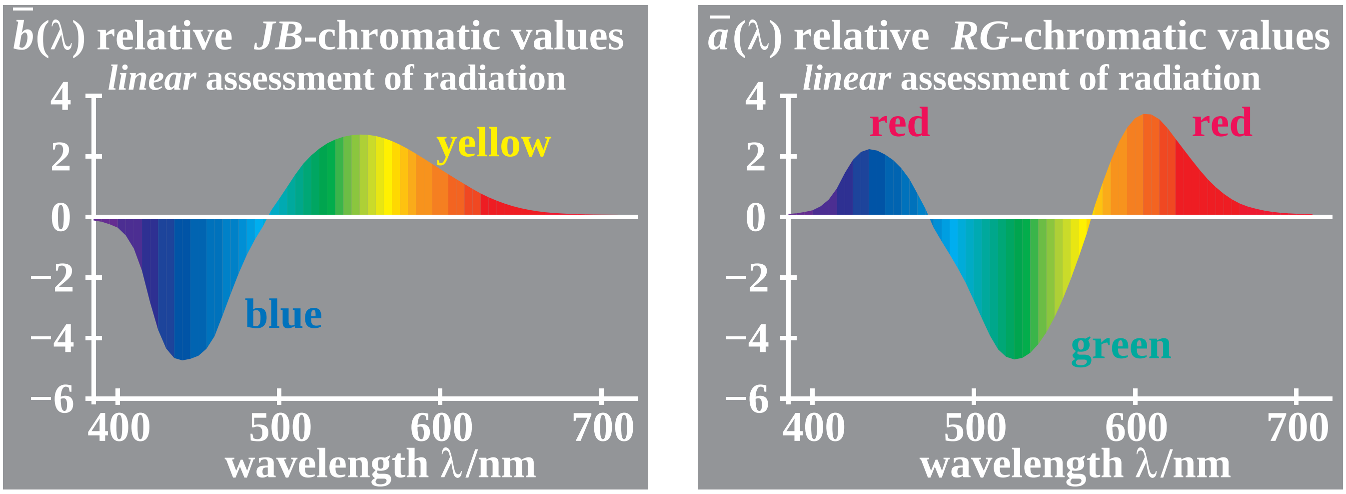

E8141−11 E8140−81

Figure 29: Elementary colours in the spectrum according to the *Hurvich* and *Jameson* model

Fig. 29 shows the two processes blue–yellow and red–green described by a simple transformation of the CIE colour matching functions according to *Hurvich* (1981). The values in Fig. 29 are calculated from the CIE colour matching functions

$a(\lambda) = x(\lambda) - y(\lambda)$

$b(\lambda) = 0{,}4\, [\, z(\lambda) - y(\lambda)\,]$

The values of the functions $a(\lambda)$ and $b(\lambda)$ are zero at approximately the wavelength 475nm, 503nm and 575nm for Blue *B*, Green *G* and Yellow *J*.

In the following we will study other experimental results of elementary colours. There is a famous elementary hue circle of *Miescher* (1948) with 24, 96, and 400 hue steps. The circle has been developed by 28 observers under daylight and CIE illuminant C has served for the calculations. The CIE colorimetric data for CIE Illuminant C are similar compared to the CIE colorimetric data for CIE illuminant D65 if the samples are non fluorescent which is the case for the samples of the *Miescher* elementary colour circle.

Four elementary colours and four intermediate colours		CIE tristimulues values and chromaticity for illuminant C and 2 degree observer				
Hue circle	**Miescher/Munsell hue**	X_C	Y_C	Z_C	x_C	y_C
Elementary Red R	08/6.0R−V5	32,53	18,11	5,32	0,5813	0,3236
red yellow R50J	05/3.7YR−V5	60,31	45,44	5,55	0,5419	0,4083
Elementary Yellow J	02/8.5Y−V5	70,52	77,82	10,18	0,4449	0,4909
yellow green J50G	23/9.5GY−V5	25,23	45,15	14,00	0,2990	0,5351
Green G	20/5.9G−V5	8,51	20,24	16,28	0,1890	0,4495
green blue G50B	17/8.5BG−V5	8,83	14,56	31,55	0,1607	0,2650
Blue B	14/5.3PB−V5	11,92	9,35	48,79	0,1701	0,1335
blue red B50R	11/7.4P−V5	16,15	8,47	30,90	0,2909	0,1526

XE350−1

Figure 30: *Miescher* elementary colour circle and correponding *Munsell* notation

Fig. 30 shows the CIE data of the *Miescher* elementary colour circle and the correponding *Munsell* colour notations.

Elementary and intermediate colours					Munsell Notation (Value 5) and dominant wavelength	
Hue	**Observer K.R.**	**G.W.**	**A.V.**	**K.M.**	**mean Munsell value and dominant wavelength**	**correction for Bezold-Brücke effect**
Red R	6.5R 700	5.8R 494c	6.0R 494c	5.8R 494c	6.0R 494c	494c 700 495c
R50J	3.75YR 592	4.2YR 591	3.5YR 593	3.7YR 592	3.7YR 592±1	590±2
Yellow J	7.5Y 575	8.5Y 574	10.0Y 572	10.0Y 572	8.5Y 574±2	572±2
J50G	10GY 542	8.75GY 550	9.0GY 548	0.5G 536	9.5GY 544±8	542±10
Green G	6.0G 502.5	5.0G 504	6.0G 502.5	6.7G 501.5	5.9G 503±2	503±2
G50B	7.5BG 488.5	8.75BG 487.5	8.0BG 488	10.0BG 486.5	8.5BG 488±2	489±2
Blue B	5.6PB 472	5.0PB 474.5	5.1PB 474	5.0PB 474.5	5.3PB 474±2	472±2
B50R	7.5P 558c	7.5P 558c	7.0P 560c	7.5P 558c	7.4P 559c±1	559±1

XE350−7

Figure 31: Experimental *Munsell* colour notation and dominant wavelength for elementary colours

Fig. 31 shows the experimental *Munsell* colour notation and the dominant wavelength for the elementary and intermediate colours of the *Miescher* elementary colour circle according to *Richter* (1969). In the following vision model for the three elementary colours *B, G* and *J* the dominant wavelength 475nm, 525nm and 575nm are used. In a following improved model it is intended to change the dominant wavelength 525nm of Green *G* to the experimental dominant wavelength around 503nm.

Elementary colour and CIE illuminant		CIELAB data, CIE tristimulus values and CIE chromaticity for CIE standard illuminants D65 and D50 and 2 degree observer									
CIE-test colour	**Ill.**	L^*	a^*	b^*	C^*_{ab}	h_{ab}	X	Y	Z	x	y
09, Red R	D65	40,04	58,98	28,32	65,43	25,7	20,64	11,27	4,34	0,5693	0,3110
10, Yellow J		81,30	−2,99	71,82	71,89	92,4	54,89	59,01	12,02	0,4359	0,4686
11, Green G		52,27	−42,40	13,64	44,54	162,2	12,15	20,38	15,34	0,2538	0,4258
12, Blue B		30,52	1,21	−46,35	46,37	271,5	6,24	6,45	27,59	0,1550	0,1601
09, Red R	D50	41,88	62,00	31,82	69,69	27,2	23,31	12,42	3,24	0,5982	0,3188
10, Yellow J		81,97	1,81	71,59	71,61	88,5	58,84	60,24	9,50	0,4576	0,4685
11, Green G		51,62	−41,12	11,52	42,70	164,4	12,10	19,81	11,95	0,2759	0,4515
12, Blue B		29,20	−5,28	−49,34	49,62	263,9	5,25	5,92	21,25	0,1621	0,1825

XE350−3

Figure 32: Colorimetric data of the CIE-test colours no. 9 to 12 which represent the four elementary colours

Fig. 32 shows the colorimetric data of the CIE-test colours no. 9 to 12 which are good approximations of the four elementary colours for the CIE illuminants D65 and D50.

The spectral data of the CIE-test colours are defined in CIE 13.3. There are real samples from BAM and other sources which approximate the CIE spectral reflectance. Additionally metameric samples for D65 are available, e. g. the metameric ISO/IEC-test charts according to ISO/IEC 15775 include the CIE-test colours which are produced with standard offset printing inks.

In image technology the CIELAB hue angles h_{ab} = 27, 92, 158, 273 for RJGB are used to define the elementary hues and to produce these hues. For a real printer on 10 pages the six device colour hues (OYLCVM) and the four elementary hues (RJGB) are produced. For this printer example see the file (350 kByte, 10 pages).

http://www.ps.bam.de/VE39/10L/L39E00NP.PDF

The CIELAB hue angles h_{ab} are given in the output for both: the six basic device colours *OYLCVM* and the four CIE-elementary hues *RJGB* approximately produced by the printer with the name FRS06

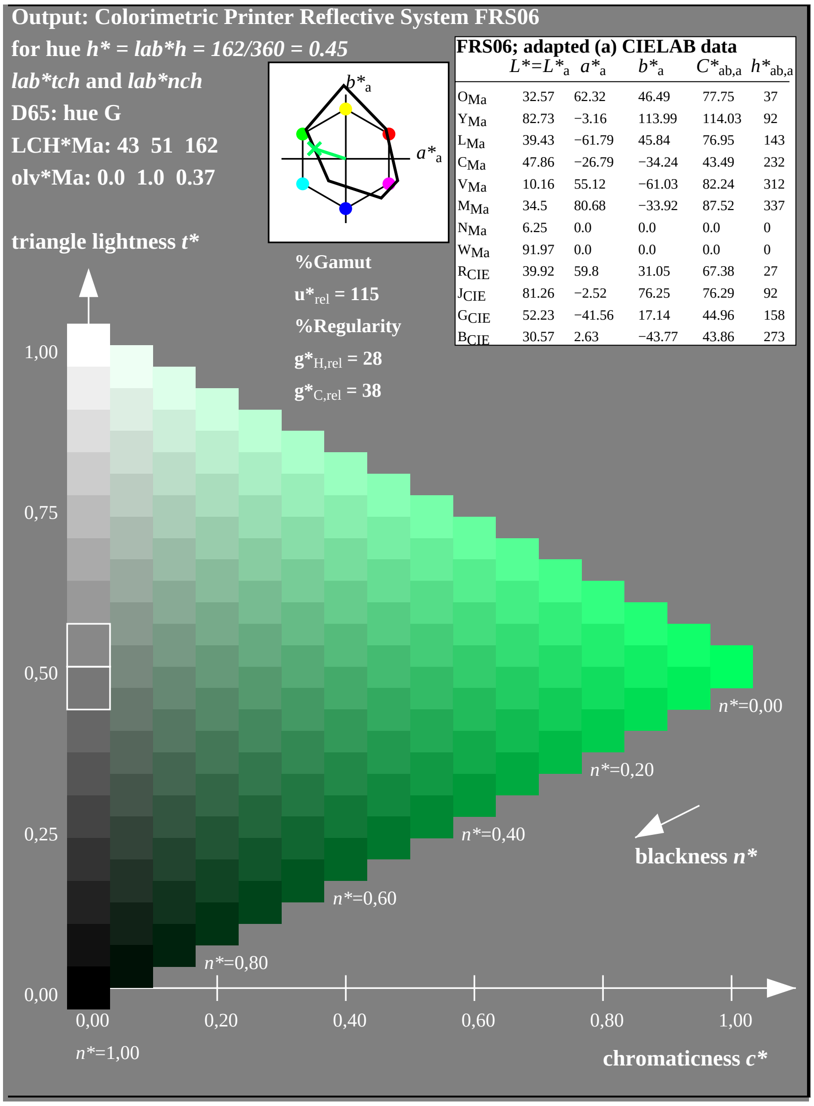

Figure 33: 16 step colour series in a hue triangle with the elementary hue green

Fig. 33 shows the 16 step colour series in a hue triangle with the elementary hue green of the CIELAB hue angle h_{ab} = 162 degrees. The three 16 step series black–white, white–green and green–black should be visually equally spaced. This is for different devices often not the case. ISO/IEC TR 19797 describes a method to improve the output according to this goal.

A hue triangle includes the colour attribute relative whiteness, relative chromaticness and relative blackness which are all on a scale between 0 and 1. According to *Ostwald* (1930) there is a colorimetric relation

whiteness + blackness + chromaticness = 1

For the colorimetric attribute “relative blackness” one can try to find a relation compared to all the achromatic and chromatic signals which we have plotted and which we will plot in the next sections.

The *Swedish Natural Colour System NCS* (1982) has choosen the three relative colour attributes “elementary hue”, “blackness” and “chromaticness” as primary colour attributes. One can compare these attributes with the notations of the *Munsell* color order system: Hue, Chroma and Value. The definitions of triangle lightness *t** and blackness *n** which are used in Fig. 33 are different compared to the definition of CIE lightness *L**, compare Richter (2006a)

It is an open question if we can use the basic coordinates of the intended colour vision model to describe the *NCS* coordinates in addition to the CIELAB coordinates which represent the main coordinates of the *Munsell* system.

7. More symmetry properties of the colour vision model

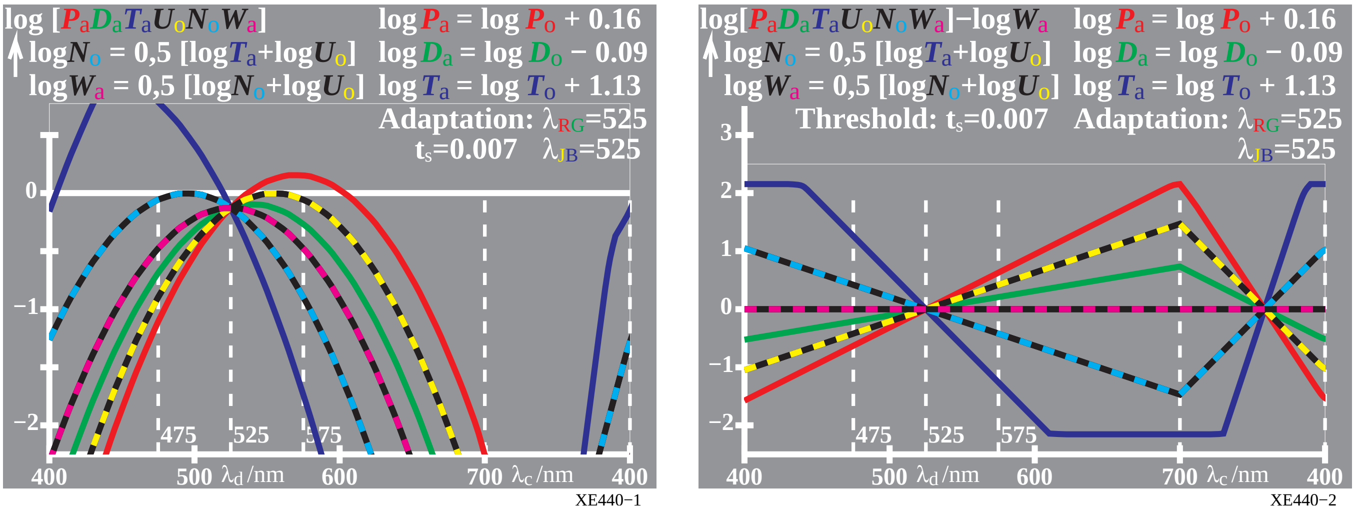

Figure 34: Sensitivities U_o, N_o, W_a, P_a, D_a, T_a *(left)* and excitations e_{xW} *(right)* for $\lambda_{RG}=\lambda_{JB}=525$nm

Fig. 34 is equal to Fig. 20 and shows the sensitivities U_o, N_o, W_a, P_a, D_a, T_a *(left)* and excitations e_{xU} *(right)* for red–green (RG-) adaptation to 525nm.

There are a simple relation:

$\log N_o(\lambda) = 0{,}5\ [\ \log T_a(\lambda) + \log U_o(\lambda)\ ]$

Searching for symmetry there is a similar symmetric relation:

$\log U_o(\lambda) = 0{,}5\ [\ \log T'_a(\lambda) + \log N_o(\lambda)\ ]$

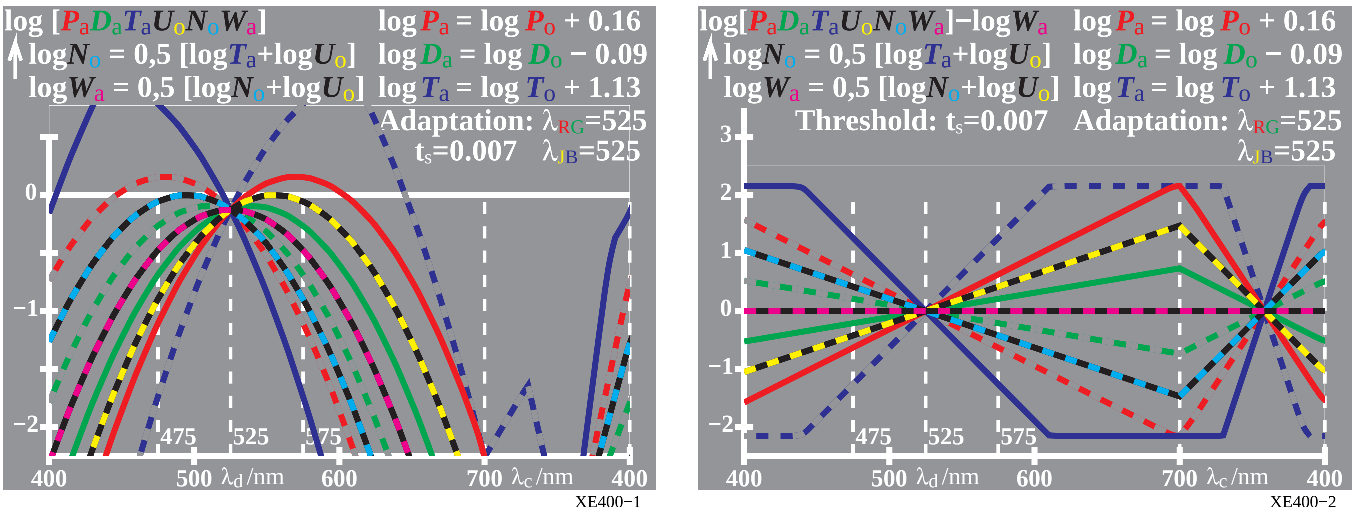

Figure 35: 9 sensitivities U_o, N_o, W_a, P_a, D_a, T_a, P'_a, D'_a, T'_a *(left)* and excitations e_{xW} *(right)* for $\lambda_{RG}=\lambda_{JB}=525$nm

Fig. 35 shows 9 sensitivities U_o, N_o, W_a, P_a, D_a, T_a, P'_a, D'_a, T'_a*(left)* and excitations *(right)* for the RG- and JB-adaptation to 525nm. The sensitivity T'_a with a dash (') is defined in the above equation. It seems not impossible that the "dash-sensitivity" is calculated by the simple equation above for T'_a and with similar equations for P'_a, D'_a.

If we look at the excitations in the right part of Fig. 35 we now realize complete symmetry:

1. between the lines above and below the zero line ("mesopic excitation") and
2. between the slopes on the wavelength scale larger and smaller compared to 525nm

If there is a dynamic range limit (threshold t_s = 0.007) then the excitation e_{TW} saturates below 350nm and above 610nm. This range of the mesopic excitation e_{TW} is larger compared to the photopic excitation e_{TU} in Fig. 19.

However both the mesopic excitation e_{TW} and the photopic excitation e_{TU} may play some minor role compared to e_{NW} which is **not** saturated in the whole visual range. Additionally neither the mesopic excitation e_{PW} nor the mesopic excitation e_{DW} is saturated in the whole visual range.

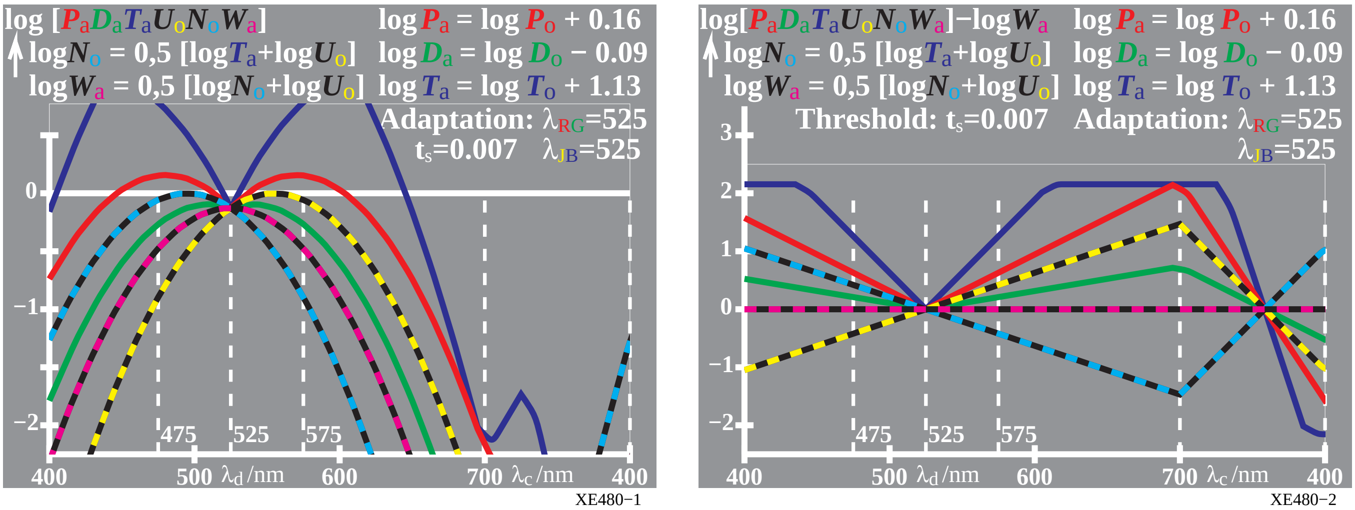

Figure 36: Active sensitivities P_a, D_a, T_a, P'_a, D'_a, T'_a *(left)* and excitations e_{xW} *(right)* for $\lambda_{RG}=\lambda_{JB}$=525nm

Fig. 36 shows the 6 "active" sensitivities P_a, D_a, T_a, P'_a, D'_a, T'_a, and U_o, N_o, W_a *(left)* and the mesopic excitations e_{xW} *(right)* for the RG-adaptation to 525nm. We have to define the term "active sensitivities". In Fig. 21 we showed that for the BJ-process for example only the blue signals which are larger compared to the achromatic system play a considerable role for luminance and chromatic discrimination of the blue colours. If we look at the excitations in Fig. 36 *(right)* then additionally all the negative parts below the red-black zero line of the "active" sensitivities are deleted. In Fig. 36 we have not deleted the negative part of *(U/W)* and *(N/W)* *(yellow–black and cyan–black line)*.

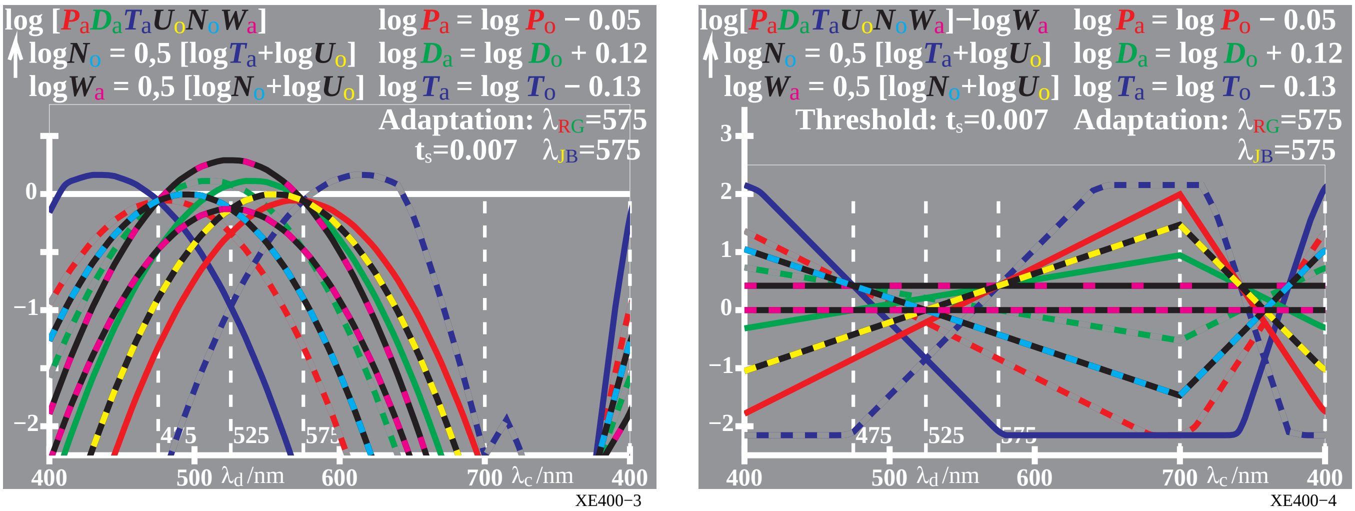

Figure 37: Sensitivities U_o, N_o, W_a, P_a, D_a, T_a, P'_a, D'_a, T'_a *(left)* and excitations e_{xW} *(right)* for $\lambda_{RG}=\lambda_{JB}$=575nm

Fig. 37 shows 9 sensitivities U_o, N_o, W_a, P_a, D_a, T_a, P'_a, D'_a, T'_a, and U_o, N_o, W_a, H_a *(left)* and the mesopic excitations *(right)* for the RG-and JB-adaptation to 575nm, which indicates complete adaptation to 575nm. Compared to Fig. 36 both in the red–green and yellow–blue direction the adaptation has changed from 525nm to 575nm. The RG-properties are similar to the properties of Fig. 18. The sensitivity H_a is defined by a vertical shift on W_a defined by λ_{RG} = 575nm.

As known from the *von Kries* theory of chromatic adaptation the three cone sensitivities will change. Instead of three here six cone sensitivities change and the most surprising change is the change of the two sensitivities T_a and T'_a.

As a result the two opponent elementary colours Yellow *J* and Blue *B* which are defined by the dominant wavelength 575nm and 475nm have a zero red–green signal. If elementary Yellow *J* and Blue *B* mix by the colorimetry to White *W* then we can expect additionally a zero red–green signal for the achromatic white and grey colours.

One must realize that a change of both $U_o(\lambda)$ and $N_o(\lambda)$ is not necessary. Only the weighting of $P_a(\lambda)$ and $D_a(\lambda)$ and $P'_a(\lambda)$ and $D'_a(\lambda)$ changes according to the equations

$$\log U_o(\lambda) = 0{,}5\ [\ \log P_a(\lambda) + \log D_a(\lambda)\ ]$$

$$\log N_o(\lambda) = 0{,}5\ [\ \log P'_a(\lambda) + \log D'_a(\lambda)\ ]$$

For *RG*-adaptation to 525nm it is valid

$$\log P_a(\lambda) = \log P_o(\lambda) + 0{,}16$$

$$\log D_a(\lambda) = \log D_o(\lambda) - 0{,}09$$

and for *RG*-adaptation to 575nm it is valid

$$\log P_a(\lambda) = \log P_o(\lambda) - 0{,}05$$

$$\log D_a(\lambda) = \log D_o(\lambda) + 0{,}12$$

Dependent on the *RG*-adaptation wavelength (λ_{RG} >= 525 nm) the following equation allow to determine the constants in the above equations. For any *RG*-adaptation the excitations $e_{PU}(\lambda_{RG})$ and $e_{DU}(\lambda_{RG})$ are equal

$$e_{PU}(\lambda_{RG}) = e_{DU}(\lambda_{RG})$$

or

$$\log [\ P_a(\lambda_{RG}) \,/\, U_a(\lambda_{RG})\ ] = \log [\ D_a(\lambda_{RG}) \,/\, U_o(\lambda_{RG})\ ]$$

or

$$\log P_a(\lambda_{RG}) = \log D_a(\lambda_{RG})$$

or

$$\log P_o(\lambda_{RG}) + a_P = \log D_o(\lambda_{RG}) + a_D$$

Together with

$$\log U_o(\lambda_{RG}) = 0{,}5\ [\ \log P_a(\lambda_{RG}) + \log D_a(\lambda_{RG})\ ]$$

$$\log U_a(\lambda_{RG}) = \log U_o(\lambda_{RG})$$

which leads to

$$\log U_o(\lambda_{RG}) = 0{,}5\ [\ \log P_o(\lambda_{RG}) + a_P + \log D_o(\lambda_{RG}) + a_D\ ] = 0{,}5\ [\ 2\ \{\ \log P_o(\lambda_{RG}) + a_P\ \}\ ] = \log P_o(\lambda_{RG}) + a_p$$

or

$$a_P = -\ [\ \log P_o(\lambda_{RG}) - \log U_o(\lambda_{RG})\ ] \qquad \lambda_{RG} >= 525 \text{ nm}$$

$$= -\log [\ P_o(\lambda_{RG}) \,/\, U_o(\lambda_{RG})\ ] = -\ e_{PU}(\lambda_{RG})$$

$$a_D = -\ [\ \log D_o(\lambda_{RG}) - \log U_o(\lambda_{RG})\ ]$$

$$= -\log [\ D_o(\lambda_{RG}) \,/\, U_o(\lambda_{RG})\ ] = -\ e_{DU}(\lambda_{RG})$$

Therefore the chromatic *RG*-adaptation to any wavelength λ_{RG} is only a shift by a constant which is defined by the excitations $e_{PU}(\lambda_{RG})$ or $e_{DU}(\lambda_{RG})$.

Because of the symmetry of the model on the wavelength scale compared to 525nm there are the following corresponding equations for λ'_{RG} = 475nm:

$$a_{P'} = -\ [\ \log P'_o(\lambda'_{RG}) - \log N_o(\lambda'_{RG})\ ] \qquad \lambda'_{RG} < 525 \text{ nm}$$

$$= -\log [\ P'_o(\lambda'_{RG}) \,/\, N_o(\lambda'_{RG})\ ] = -\ e_{PN}(\lambda'_{RG})$$

$$a_{D'} = -\ [\ \log D_o(\lambda'_{RG}) - \log N_o(\lambda'_{RG})\ ]$$

$$= -\log [\ D_o(\lambda'_{RG}) \,/\, N_o(\lambda'_{RG})\ ] = -\ e_{DN}(\lambda'_{RG})$$

Similar equations are necessary for the yellow–blue direction.

$$\log W_a(\lambda) = 0{,}5\ [\ \log U_o(\lambda) + \log N_o(\lambda)\ ]$$

$$\log H_a(\lambda) = \log W_a(\lambda) + a_T$$

$$\log H_a(\lambda_{RG}) = \log U_o(\lambda_{RG})$$

$$\log H_a(\lambda_{RG}) = \log W_a(\lambda_{RG}) + a_T$$

it follows

$$a_T = \log H_a(\lambda_{RG}) - \log W_a(\lambda_{RG}) = \log [\ U_o(\lambda_{RG}) \,/\, W_a(\lambda_{RG})\ ]$$

$$= \log U_o(\lambda_{RG}) - 0{,}5\ [\ \log U_o(\lambda_{RG}) + \log N_o(\lambda_{RG})\ ]$$

$$= 0{,}5 \log U_o(\lambda_{RG}) - 0{,}5 \log N_o(\lambda_{RG})$$

$= 0{,}5 \log U_o(\lambda_{RG}) / N_o(\lambda_{RG})$

$= 0{,}5\ e_{UN}(\lambda_{RG})$

Therefore for any yellow–blue adaptation

$\log H_a(\lambda_{RG}) = \log W_a(\lambda_{RG}) + 0{,}5\ e_{UN}(\lambda_{RG})$

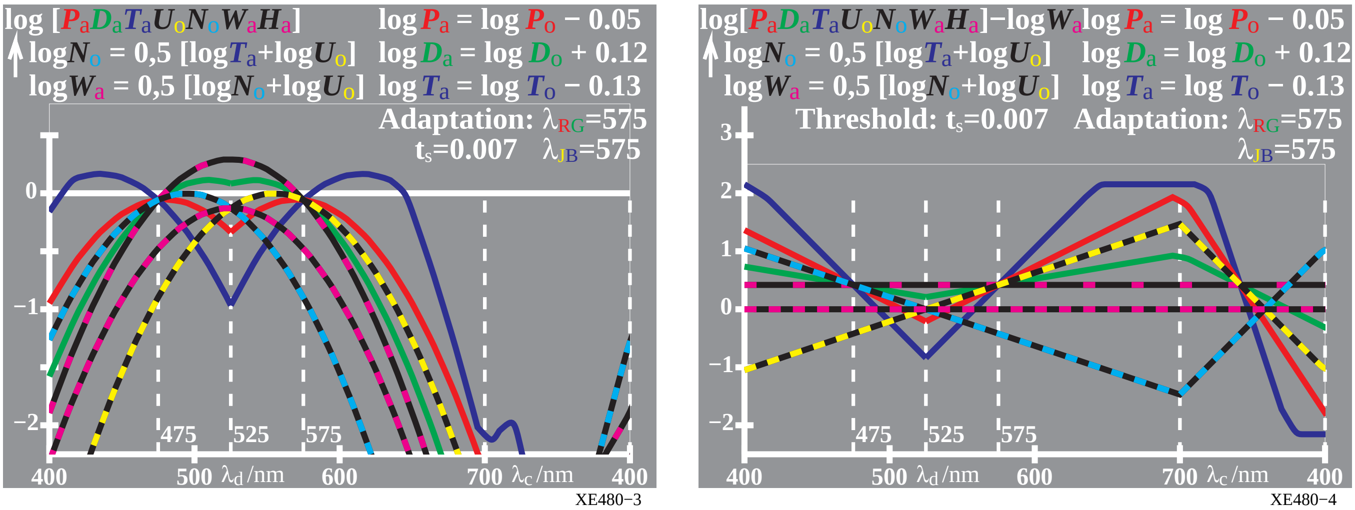

Figure 38: Active Sensitivities P_a, D_a, T_a, P'_a, D'_a, T'_a *(left)* and excitations e_{xW} *(right)* for $\lambda_{RG}=\lambda_{JB}$=575nm

Fig. 38 shows the 6 active sensitivities P_a, D_a, T_a, P'_a, D'_a, T'_a, and U_o, N_o, W_a, H_a *(left)* and the mesopic excitations *(right)* for the RG- and JB–adaptation to 575nm

8. Cone excitation diagram and chromatic adaptation

8.1 Excitation diagram in mesopic units

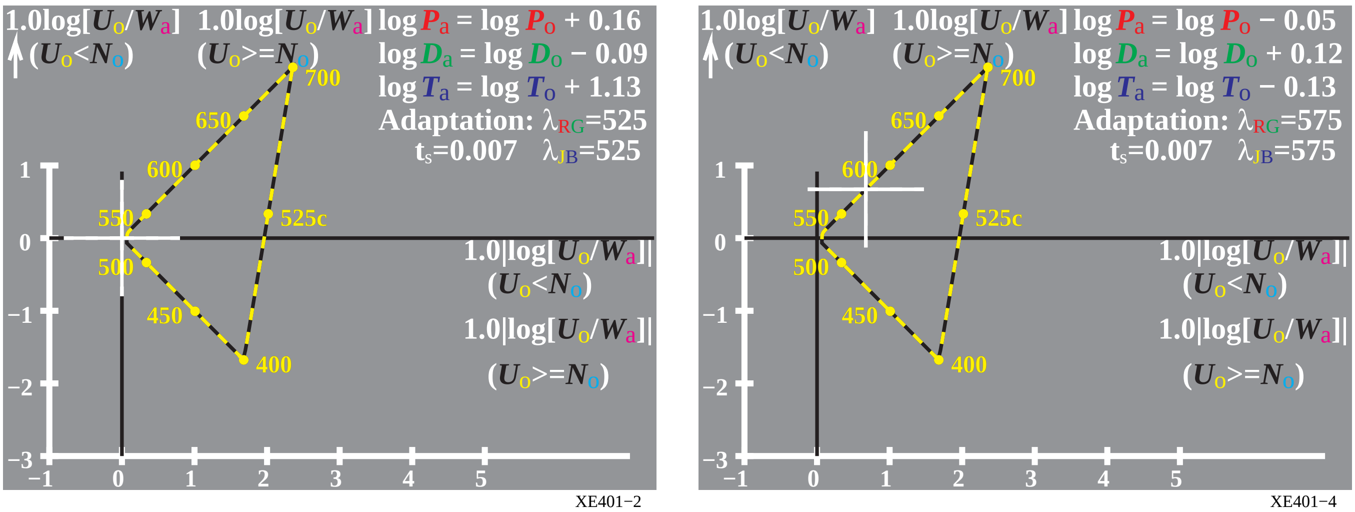

Figure 39: Cone excitation diagrams in mesopic units for adaptations $\lambda_{RG}=\lambda_{JB}$=525nm and $\lambda_{RG}=\lambda_{JB}$=575nm

Fig. 39 shows cone excitation diagrams in mesopic units for the two adaptations $\lambda_{RG}=\lambda_{JB}$=525nm *(left)* and $\lambda_{RG}=\lambda_{JB}$=575nm *(right)*. The vertical and horizontal axis parameters are the same with the important difference that the absolute value is used in the horizontal direction

$a'(\lambda) = |\log [\,U_o(\lambda) / W_a(\lambda)\,]\,|$

$= |\,e_{UW}(\lambda)\,|$

$b'(\lambda) = \log [\,U_o(\lambda) / W_a(\lambda)\,]$

$= e_{UW}(\lambda)$

The background excitation of the wavelength λ_{RG}=λ_{JB}=525nm *(left)* and λ_{RG}=λ_{JB}=575nm *(right)* is shown by a white mark. It is important to realize that the shape and form of the diagram [$a'(\lambda)$, $b'(\lambda)$] is **independent** of chromatic adaptation. Therefore the chromatic adaptation formula is only a shift between the sample and the background excitation, for example if a' is the excitation of the sample and a'_n is the excitation of the background, then it is valid for any background (Index n, e. g. D65 or D50)

$$a' - a'_n = a'(D65) - a'_{D65}$$

$$b' - b'_n = b'(D65) - b'_{D65}$$

If the two background chromaticities are D65 and D50 then it is valid:

$$a'(D65) - a'_{D65} = a'(D50) - a'_{D50}$$

$$b'(D65) - b'_{D65} = b'(D50) - b'_{D50}$$

Therefore the description of chromatic adaptation is very simple and looks similar compared to the shift in the colour space CIELUV 1976. The similar equations in CIELUV are:

$$u'(D65) - u'_{D65} = u'(D50) - u'_{D50}$$

$$v'(D65) - v'_{D65} = v'(D50) - v'_{D50}$$

Richter (1980) has developed similar equations for the CIELAB space (compare Fig. 12):

$$a'(D65) - a'_{D65} = a'(D50) - a'_{D50}$$

$$b'(D65) - b'_{D65} = b'(D50) - b'_{D50}$$

with (compare Fig. 12)

$$a' = 0{,}2191\ [\ x / y\ ]^{1/3}$$

$$b' = -\ 0{,}08376\ [\ z / y\ ]^{1/3}$$

Additionally the CIELAB chroma components can be calculated by (compare Fig. 12)

$$a^* = [\ a' - a'_n\ ]\ Y^{1/3}$$

$$b^* = [\ b' - b'_n\ ]\ Y^{1/3}$$

As a result we can expect that we can describe CIELAB chroma a^* and b^* by the above logarithmic excitation difference instead of the cube root chromaticity difference.

For the exact calculation of CIELAB chroma a^* and b^* a multiplication of the cube root chromaticity difference and the cube root of the luminance factor ($Y^{1/3}$) is necessary. We can use the logarithmic excitation difference multiplied by ($Y^{1/3}$) for a first approximation of CIELAB chroma a^* and b^*. A much better approximation of visual experimental data should use the Q-function instead of ($Y^{1/3}$). The Q-function has the important S-shape property as function of x_r = log [L / L_b] = log L_r.

There are different method to test the new symmetric colour vision model, for example can we study a monochromatic blue. For example with the monochromatic wavelength λ = 475nm and a luminance of 100 cd/m^2 in a grey background of the same luminance. Then the following basic difference is predicted:

1. CIELAB calculates a very high chroma.

2. The colour vision model calculates a chroma which is approximately zero.

The reasons for both contrary results are very different:

1. CIELAB chroma increases infinitely with $Y^{1/3}$.

2. For monochromatic blue the luminance of the **chromatic threshold** is **four log units below** the luminance of the grey surround and **two log units below** the **achromatic threshold**. Therefore we can expect that the chroma C^*_{ab} of the monochromatic blue reaches its maximum 2 log units below the background luminance and saturates at the background luminance. This leads to a zero chroma at the background luminance.

Therefore CIELAB seems completely wrong with the unlimited increase in chroma as function of the cube root of the luminance factor. The Q-function includes a saturation effect and predicts a chroma of zero for samples with about the relative luminance L_r of the grey background.

Remark: Because of the variable threshold range this zero point may also occur one log unit above the background luminance.

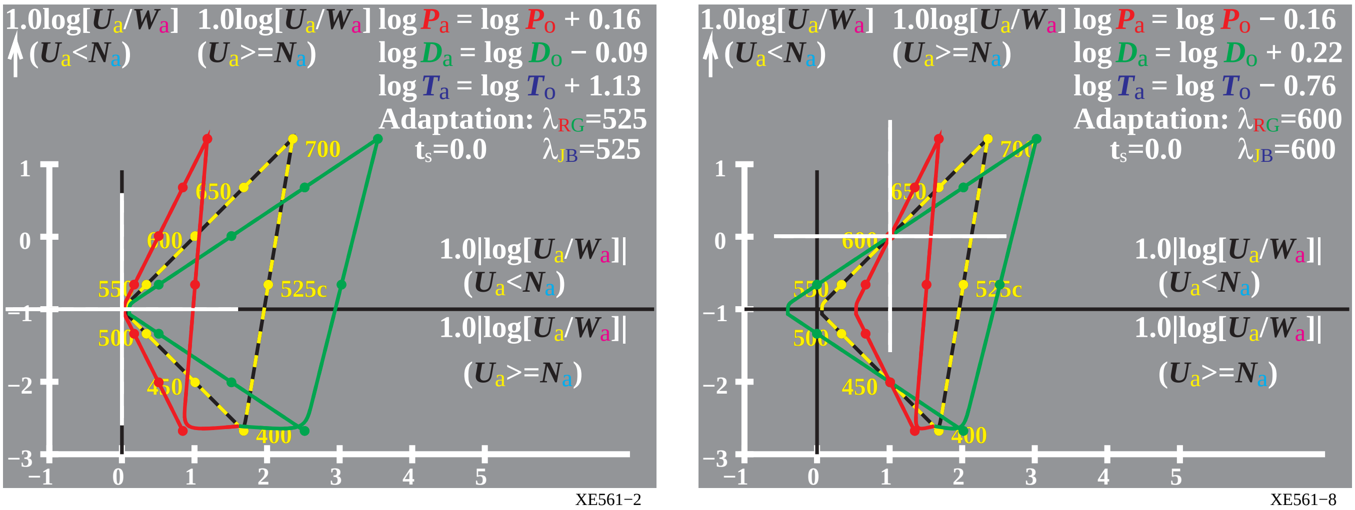

Figure 40: Three excitation diagrams in mesopic units for adaptations $\lambda_{RG}=\lambda_{JB}$=525nm and $\lambda_{RG}=\lambda_{JB}$=575nm

Fig. 40 shows three excitation diagrams in mesopic units for the two adaptations $\lambda_{RG}=\lambda_{JB}$=525nm *(left)* and $\lambda_{RG}=\lambda_{JB}$=575nm *(right*). For the vertical and horizontal axis the same mesopic excitation $e_{UW}(\lambda)$ is used with the important difference that in the horizontal direction the absolute value | $e_{UW}(\lambda)$ | is used.

Additionally for $\lambda_{RG}=\lambda_{JB}$=525nm *(left)* the “red” excitation $e_{PU}(\lambda)$ is subtracted on the horizontal axis for the red diagram and the “green” excitation $e_{DU}(\lambda)$ is added on the horizontal axis for the green diagram *(left)*.

Similar additionally for $\lambda_{RG}=\lambda_{JB}$=575nm *(right*) the “red” excitation $e_{PU}(\lambda)$ is subtracted on the horizontal axis for the red diagram and the “green” excitation $e_{DU}(\lambda)$ is added on the horizontal axis for the green diagram *(right)*.

In both cases the white cross shows the excitation of the background 525nm *(left)* and 575nm *(right).* In both cases the two mesopic excitations |$e_{UW}(\lambda)$ | and $e_{UW}(\lambda)$ *(yellow–black colour)* are cutting by the “red” and the “green” excitations at the background.

Interpretations of these kind of excitation diagrams have to be developed further.

8.2 Model and *Evans* G0-colours in a monochromatic background $\lambda_{RG} = \lambda_{JB}$ = 525nm

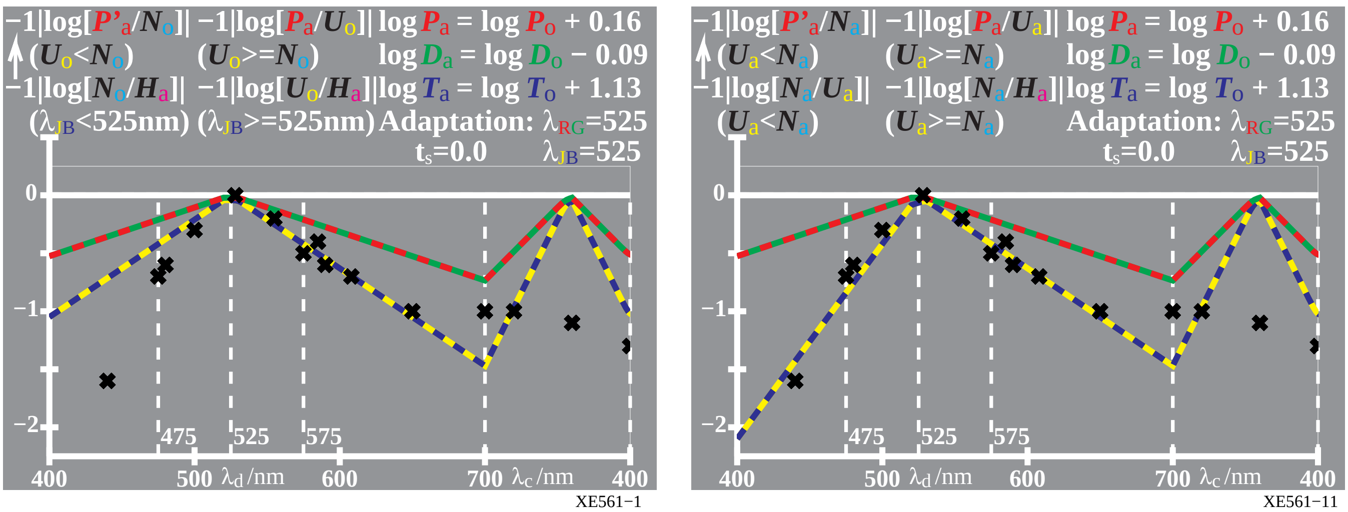

Figure 41: Model and *Evans* G0-colours in a monochromatic background $\lambda_{RG} = \lambda_{JB}$ = 525nm

Fig. 41 shows the model and *Evans* G0-colours in a monochromatic background $\lambda_{RG} = \lambda_{JB}$ = 525nm. The G0 colours are the colours of relative blackness n^* = 0 which are shown in Fig. 33 for an achromatic white background.

There is a first model with two mesopic exitations $e_{NH}(\lambda)$ *for* $U_o < N_o$ *and* $e_{UH}(\lambda)$ *for* $U_o >= N_o$ *(left)* and a second model with one photopic excitation $e_{NU}(\lambda)$ *for* $U_o < N_o$ and the same mesopic excitation $e_{UH}(\lambda)$ *for* $U_o >= N_o$ *(right).*

The second model *(right)* fits the *Evans* (1974) data in the whole range much better. Therefore the use of some cone excitation in **photopic** units for λ < 525nm is necessary for the description of the experimental results below 525nm.

Remark: The description for the purple colours has to be studied further. At the moment we do not know how to handle the change of the sign (absolute values) in the purple range. There is a possibility to interpolate between the sensitivities or excitations and to use for this the data at the two wavelength 400nm and 700nm.

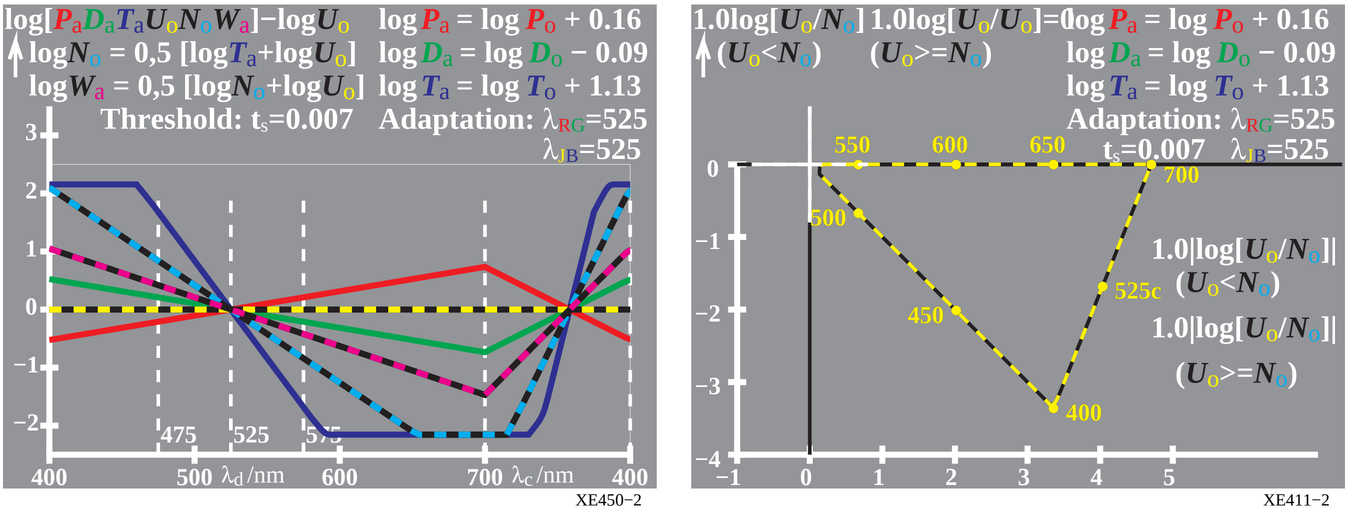

Figure 42: Cone excitations *(left)* and excitation diagram *(right)* in photopic units for λ_{RG}=λ_{JB}=525nm

Fig. 42 shows cone excitations *(left)* and excitation diagrams *(right)* in photopic units for the adaptation λ_{RG}=λ_{JB}=525nm as function of wavelength *(left)* and in two dimensions *(right)*. The parameters of the vertical and horizontal axis could be always equal for example

log [$N_o(\lambda)$ / $U_o(\lambda)$]   for any U_o, N_o

or different. We have chosen two equations:

log [$N_o(\lambda)$ / $U_o(\lambda)$]   for $U_o < N_o$

log [$N_o(\lambda)$ / $U_o(\lambda)$] = 0   for $U_o >= N_o$

Again the absolute value | log [$N_o(\lambda)$ / $U_o(\lambda)$] | is used for any U_o and N_o in the horizontal direction. The reason of this choice is the success in Fig. 41 for the description of the *Evans* G0-colours with excitations below 525nm in photopic units. Therefore we use in Fig. 42 in horizontal and vertical direction:

$a'(\lambda)$ = | log [$U_o(\lambda)$ / $N_o(\lambda)$] | = | – log [$N_o(\lambda)$ / $U_o(\lambda)$] | for any U_o, N_o

$b'(\lambda)$ = log [$U_o(\lambda)$ / $N_o(\lambda)$] for $U_o < N_o$

= 0   for $U_o >= N_o$

A more simple choice is (not plotted here)

$a'(\lambda)$ = | log [$U_o(\lambda)$ / $N_o(\lambda)$] | = | – log [$N_o(\lambda)$ / $U_o(\lambda)$] | for any U_o, N_o

$b'(\lambda)$ = log [$U_o(\lambda)$ / $N_o(\lambda)$]   for any U_o, N_o

The two coordinates define a symmetric photopic excitation diagram which is similar compared to the mesopic excitation diagram in Fig. 40.

9. Future Work

In future the vision model of this paper will be applied to the following data:

1. Scaling data of the *Munsell* colour order system.
2. Scaling data of the *OSA* colour order system.
3. Scaling data of the *NCS* colour order system and data with *NCS* elementary hue, *NCS* blackness and *NCS* chromaticness.
4. Threshold data and colour differences for adjacent colours, e. g. the data available for CIEDE2000.
5. *Evans* Go-colours for different chromatic adaptation.
6. Data of achromatic and chromatic threshold.

The basic new properties of the vision model may allow to improve the CIELAB formula which has been developed for surface colours. An improved formula should describe experimental data for a larger visual luminance and chromaticity range and for different adaptation conditions.

10. References

CIE 170-1:2006, Fundamental chromaticity diagram with physiological axes - Part 1
CIE 15: 2004, Colorimetry

Evans, R. M. (1974), The perception of colour, JOHN Wiley, New York, ISBN 0-471-24785-5, 248 pages

Goethe, J. W. (1800), Die Farbenlehre

ISO/IEC 15775:1999, Information Technology – Office Systems – Method for specifying image reproduction of colour copying machines by analog test charts – Realisation and application, Editor: K. Richter.

ISO/IEC TR 19797:2004, Information Technology – Office Systems – Device output of 16-step colour scales, output linearization method (LM) and specification of the reproduction properties, Editor: K. Richter, For Information and test charts according to ISO/IEC TR 19797 see
http://www.ps.bam.de/19797T

ISO/IEC TR 24705:2005, Information Technology – Office Systems – Method of specifying image reproduction of colour devices by digital and analog test charts, Editor: K. Richter, For Information and test charts according to ISO/IEC TR 24505 see
http://www.ps.bam.de/24705T

Holtsmark, T. and Valberg, A. (1969), Colour discrimination and hue, Nature, Volume 224, October 25, p. 366-367

Hurvich, Leo. M (1981), Colour Vision, Sinauer Associates Inc, Sunderland, Massachusetts, ISBN 0 87893-336-0

Miescher, K. (1969), The natural colour conception serving as base for elementary colour teaching, AIC Colour 69, Stockholm, Musterschmidt, p. 1231-1241

Natural Colour System *NCS* (1982), Svensk Standard SS 01 91 0:1982, Colour notation system – SS 01 91 01:1982, CIE tristimulus values and trichromatic co-ordinates for some 16 000 colour notations according to SS 01 91 00 – SS 01 91 02:1982, Colour atlas – SS 01 91 02:1982, CIE tristimulus values and chromaticity co-ordinates for colour samples in SS 01 91 02

Ostwald, W, (1923), Physikalische Farbenlehre, Leipzig, Unesma
Ostwald, W, (1930), Die Farbenfibel, Leipzig, Unesma

Richter, K. (1969), Antagonistische Signale beim Farbensehen und ihr Zusammenhang mit der empfindungsgemässen Farbordnung, Disserattion, Universität Basel

Richter, K. (1971), (1971), Description of colour attributes and colour differences, In: Color Metrics, AIC, Soesterberg, TNO, 134-146

Richter, K., BAM-Research Report no. 61 (1979), Beschreibung von Problemen der höheren Farbmetrik mit Hilfe des Gegenfarbensystems, 99 pages, ISSN 0172-7613

Richter, K. (1980), Cube root colour spaces and chromatic adaptation, Color Res. and Appl. 5, no. 1, S. 25-43

Richter, K., BAM-Research Report no. 115 (1985), Farbempfindungsmerkmal Elementarbuntton und Buntheitsabstände als Funktion von Farbart und Leuchtdichte von In- und Umfeld, 118 pages, ISBN 3-88314-420-7

Richter, K. (1996), Computergrafik and Farbmetrik, Farbsysteme, PostScript, geräteunabhängige CIE-Farben, VDE-Verlag, Berlin, ISBN 3-8007-1775-1, 288 pages including CD-ROM and about 500 pictures in colour, see http://www.ps.bam.de/buch

Richter, Klaus (2005a), Relative Colour Image Technology (RCIT) and RLAB lab* (2005) Colour Image Encoding, see (70 pages, 850 kByte)

http://www.ps.bam.de/RLABE.PDF

Richter, K. (2005b), Linear relationship between CIELAB and device coordinates for Colorimetric Image Technology (CIT), see (140 kByte, 6 pages)

http://www.ps.bam.de/CIE05.PDF

Richter, K. (2006a), Device dependent linear relative CIELAB data *lab** and colorimetric data for corresponding colour input and output on monitors and printers, CIE Symposium, 75 years colorimetric observer, Ottawa/Canada, 2006, 6 pages, to be published by the CIE in the Symposium-Proceedings.

Richter, K. (2006b), Relation of *Weber law* and *Stevens law* at achromatic threshold, see (11 pages, 200 kByte)

http://www.ps.bam.de/BAMAT.PDF

Valberg, A. and Holtsmark, T. (1971), Similarity between JND-curves for complementary optimal colours, In: Color Metrics, AIC, Soesterberg, TNO, 58-68

Valberg, Arne (2005), Light – Vision – Color, John Wiley & Sohn, 462 pages

Witt, J. (2006), Farbmetrische Methoden zur Herstellung von Prüfvorlagen für Farbkopierer, Farbscanner und Farbmonitore, Dissertation, TU Berlin, Fakultät IV, Elektrotechnik und Informatik, 177 pages